

NPS ARCHIVE

1997

SLIGER, D.

DUDLEY KNOX LIBRARY
NAVAL POSTGRADUATE SCHOOL
MONTEREY, CA 93943-5101

**DUDLEY KNOX LIBRARY
NAVAL POSTGRADUATE SCHOOL
MONTEREY, CA 93943-5101**

STABILITY TRANSITIONS FOR WEAKLY
COUPLED VAN DER POL OSCILLATORS

by

David M. Sliger

A thesis submitted in partial fulfillment of the
requirements for the degree of

Master of Science in Mechanical Engineering

University of Washington

HPC Archive
1997
Sliger, D.

~~Thesis~~
~~55% 35~~
~~c.1~~

TABLE OF CONTENTS

LIST OF FIGURES	iii
LIST OF TABLES	iv
CHAPTER 1: INTRODUCTION	1
THE VAN DER POL EQUATION	1
CHARACTERIZING THE VAN DER POL EQUATION	3
CHAPTER 2: SOLUTION TO THE VAN DER POL EQUATION	4
SYMMETRY IN THE VAN DER POL EQUATION.....	6
CHAPTER 3: BRIEF DESCRIPTION OF PADÉ APPROXIMANTS.....	9
WHAT IS A PADÉ APPROXIMANT?	9
WHAT ARE PADÉ APPROXIMANTS FOR?	10
CALCULATING PADÉ APPROXIMANTS	11
EXAMPLES.....	12
STABILITY OF PADÉ APPROXIMANTS	14
APPLYING PADÉ APPROXIMANTS TO PERTURBATION RESULTS	17
Large ϵ Concerns	18
Application to Coupled van der Pol Oscillators.....	18
CHAPTER 4: COUPLED OSCILLATOR ANALYSIS.....	20
PROPOSED MODEL FOR COUPLED OSCILLATORS.....	20
DERIVATION OF THE VARIATIONAL EQUATIONS.....	21
SIGNIFICANCE OF THE ZERO MEAN DAMPING SURFACE.....	23
CALCULATING THE ZMD SURFACE.....	24
FLOQUET THEORY AND STABILITY TRANSITIONS CURVES	26
CHAPTER 5: PERIODIC SOLUTIONS OF THE VARIATIONAL EQUATION.....	29
SOLUTION METHOD	29
DEALING WITH $A_0 = -1/2$	31
SOLVING FOR THE STABILITY TRANSITION CURVES	31

CONDITIONS FOR SUPPRESSING SECULARITY	32
Case 1: $A_0 = 0$	33
Case 2: $A_0 = 3/2$	34
Case 3: $A_0 = 4$	35
CHAPTER 6: SUMMARY AND FUTURE WORK	38
SUMMARY	38
FUTURE WORK	39
BIBLIOGRAPHY	41
APPENDIX A: MATHEMATICA™ CODE FOR VDP EQUATION	43
APPENDIX B: STABILITY TRANSITION CODE	49
APPENDIX C: SOLUTION TO VDP EQUATION	58
APPENDIX D : SOLUTIONS TO THE VARIATIONAL EQUATION.....	62
APPENDIX E : STABILITY TRANSITION CURVES	65

LIST OF FIGURES

<i>Number</i>	<i>Page</i>
Figure (1-1) Phase-plane for VDP Oscillator ($\epsilon=0.9$).....	2
Figure (3-1) Taylor's series and Padé approximant for $1/(1+x)$	10
Figure (3-2) Taylor's series and a [3/4] approximant to $f(x) = \frac{1}{\sqrt{1+x^2}}$	14
Figure (3-3) Power series and Padé approximant to the frequency of a van der Pol limit cycle.....	18
Figure (4-1) Padé approximant to the B_{ZMD} vs. ϵ	25
Figure (4-2) Padé approximant to the ZMD surface in 3-D parameter space.....	26
Figure (5-1) Power series and Padé approximants [16/16] to transition curves out of $A_0=0$	34
Figure (5-2) Power series and Padé approximants [12/12] to transition curves out of $A_0=3/2$	35
Figure (5-3) Power series and Padé approximants [16/16] to transition curves out of $A_0=4$	37
Figure (6-1) Stability regions for coupled VDP oscillators on the ZMD surface.....	38
Figure (6-2) Three dimensional plot of the stability transition curves along the ZMD surface.	40

LIST OF TABLES

<i>Number</i>	<i>Page</i>
Table (3-1) Condition number and loss of accuracy for Example (3-2).	15

ACKNOWLEDGMENTS

The author wishes to thank the supervisory committee for their help in guiding my research. In particular, the author wishes to acknowledge the extensive guidance provided by Dr. Duane Storti.

DEDICATION

The author wishes to dedicate this thesis to Rebecca N. Sliger in appreciation of her loving support.

CHAPTER 1: INTRODUCTION

The purpose of this thesis is to study the stability characteristics of a pair of coupled van der Pol equations. In order to fulfill this purpose, several different concepts must be discussed prior to actually looking at the behavior of the coupled equations.

The first issue to be dealt with is the van der Pol equation itself; this topic will be covered in this chapter with details of the solution to the van der Pol equation via perturbation theory given in Chapter 2.

Chapter 3 will explore the derivation, existence and computation of Padé approximants which will be used to model behaviors of the van der Pol equation and the coupled equations. If the reader is already comfortable with the characteristics of Padé approximants, Chapter 3 can be skipped.

In Chapter 4, the model for the coupled van der Pol oscillators will be examined. The scope of the problem of characterizing the stability behaviors of the coupled equations will be examined. To that end, the Zero Mean Damping (ZMD) surface will be introduced and the variational equations to the coupled oscillators will be derived. Some implications of Floquet theory on the variational equations will also be explored.

Chapter 5 will detail the solution process of the variational equation derived in Chapter 4. The stability transition curves along the ZMD surface will be introduced and the method for determining them will be presented.

Chapter 6 will summarize the results of Chapter 5 and discuss some ongoing work and computational difficulties encountered in determining the stability transition curves. Further studies will also be discussed.

THE VAN DER POL EQUATION

The van der Pol equation:

$$\ddot{u} - \epsilon(1 - u^2)\dot{u} + u = 0 \quad (1-1)$$

was introduced by Bismarck van der Pol in a paper published in 1927 [29,30] to model the non-linear resistance of certain circuits including vacuum tubes. Since that time Equation (1-1) has become a popular mathematical model for limit cycle oscillators.

A limit cycle oscillator, is an oscillator which exhibits self-sustained periodic behavior. It is non-conservative, due to a damping term, and non-linear [2,7]. In the case of the van der Pol equation, the non-linearity is also due to the damping term. Limit cycle behavior is present in many mechanical, electrical, and biological systems [3,4,5,6]. Stoker[21] and LaSalle[15] showed the existence of a unique limit cycle for Equation (1-1) for all $\epsilon > 0$. The limit cycle in the phase plane $\{u, u'\}$ is shown in Figure (1-1) for the case of $\epsilon = 0.9$.

The shape of the limit cycle for the van der Pol equation varies markedly with the value of the non-linear parameter, ϵ . For $\epsilon \ll 1$ the limit cycle is well approximated by $u = 2 \cos(t)$, while for large ϵ the limit cycle remains periodic but varies significantly from sinusoidal [10,28,29]. For large ϵ , the van der Pol equation can be used to model relaxation oscillators such as a heart beating, a clock ticking or a fish swimming [6,11,22,28].

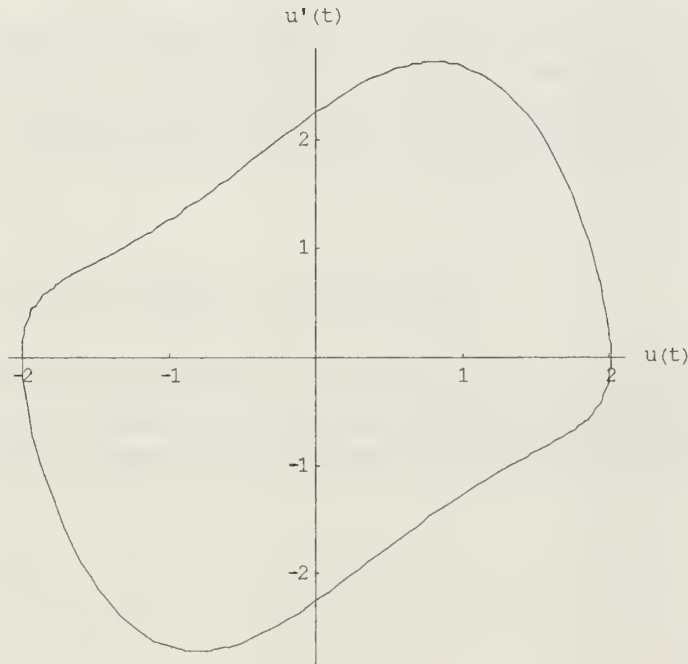


Figure (1-1) Phase-plane for VDP
Oscillator ($\epsilon = 0.9$).

Applications of relaxation oscillators is the motivation for this thesis. If the behavior of a chain of linked van der Pol equations can be characterized, it may be possible to build an electro-mechanical system which uses coupled oscillators to produce control signals for

locomotion. As an example, consider a pair van der Pol oscillators in the relaxation limit. Since $u(t)$ is characterized by a rapid transition between two relatively flat states, using the signal to drive a pair of servomechanisms may be a very inexpensive way to drive a bipedal robot. By coupling the oscillators, it may be possible to produce a smooth, responsive gait with little or no computer processing.

Another possible application for coupled van der Pol oscillators could be modeling the synapses in a fish's spine while swimming [6]. Here the chain of oscillators may be 30 or even 50 units long and modeling may be extremely complicated.

In the first step to understanding the behavior of such models, it is desirable to find the stability characteristics of the coupled equations. In this thesis, the scope will be limited to only two oscillators which could be modeled as:

$$\begin{aligned}\ddot{x} - \varepsilon(1-x^2)\dot{x} + x &= \varepsilon A(y-x) + \varepsilon B(\dot{y}-\dot{x}) \\ \ddot{y} - \varepsilon(1-y^2)\dot{y} + y &= \varepsilon A(x-y) + \varepsilon B(\dot{x}-\dot{y})\end{aligned}\tag{1-2}$$

where εA represents the displacement coupling and εB represents the velocity coupling between the two oscillators. This model was proposed by Rand and Holmes [18] and further studied by Storti and Reinhall[19,20,22,27]. In future, examining the stability of a chain of more than two oscillators could be done by extending the techniques of Storti and Reinhall and this thesis.

CHARACTERIZING THE VAN DER POL EQUATION

The first step in understanding the stability of Equations (1-2) is to develop the solution to the van der Pol equation. Equation (1-1) has been studied extensively [1, 2, 7, 8] and a simple approach to finding solutions using Lindstedt's method [14] is presented in Chapter 2.

CHAPTER 2: SOLUTION TO THE VAN DER POL EQUATION

Perturbation theory is one of the most powerful techniques used in solving non-linear differential equations in vibration theory [14,17]. In concept, perturbation theory is very simple and can be explored by examining the van der Pol equation in time t :

$$\ddot{u} - \varepsilon(1-u^2)\dot{u} + u = 0, \quad \dot{u}(0) = 0 \quad (2-1).$$

Using Lindstedt's method, rescale time and let $\tau = \omega t$. Changing variables, Equation (2-1) becomes:

$$u'' - \varepsilon(1-u^2)\omega u' + \omega^2 u = 0, \quad u'(0) = 0 \quad (2-2)$$

where the primes represent differentiation with respect to the rescaled time t . Now apply perturbation theory, by considering Equation (2-2) as a small perturbation of the linear system:

$$u'' + u = 0, \quad u'(0) = 0 \quad (2-3)$$

whose behavior is well understood. It is reasonable to assume that $u(t)$ and ω may be represented by power series in ε :

$$\begin{aligned} u(t) &= u_0(t) + \varepsilon u_1(t) + \varepsilon^2 u_2(t) + \dots \\ \omega &= 1 + \varepsilon \omega_1 + \varepsilon^2 \omega_2 + \dots \end{aligned} \quad (2-4)$$

Substituting Equations (2-4) into Equation (2-2) yields:

$$\begin{aligned} u_0'' + \varepsilon u_1'' + \varepsilon^2 u_2'' + \dots + (1 + \varepsilon \omega_1 + \varepsilon^2 \omega_2 + \dots)^2 (u_0 + \varepsilon u_1 + \varepsilon^2 u_2 + \dots) = \\ \varepsilon \left\{ 1 - (u_0 + \varepsilon u_1 + \varepsilon^2 u_2 + \dots)^2 \right\} (1 + \varepsilon \omega_1 + \varepsilon^2 \omega_2 + \dots) (u_0' + \varepsilon u_1' + \varepsilon^2 u_2' + \dots) \end{aligned} \quad (2-5)$$

Collecting like powers of ε , the first few equations become:

$$\begin{aligned}
 \varepsilon^0: \quad & u_0'' + u_0 = 0 \\
 \varepsilon^1: \quad & u_1'' + u_1 = u_0'(1 - u_0^2) - 2\omega_1 u_0 \\
 \varepsilon^2: \quad & u_2'' + u_2 = \omega_1 u_0'(1 - u_0^2) + u_1'(1 - u_0^2) - 2u_1 u_0 u_0' - 2\omega_1 u_1 - 2\omega_2 u_0 - \omega_1^2 u_0 \\
 \vdots & \vdots
 \end{aligned} \tag{2-6}.$$

These equations are then solved, in order, where the right hand side is completely fixed by the solutions to the previous equations and determining the ω_i 's and any undetermined coefficients in the earlier $u_i(t)$'s to suppress secular terms.

Secular terms are terms that if not canceled in some manner, would give solutions to the differential equation that grow with time. As an example, consider the linear Equation (2-4) with an added driving force:

$$u'' + u = \cos(t) \tag{2-7}.$$

Since the driving force matches the natural frequency, $u(t)$ will grow over time and become unbounded; the solution to Equation (2-7) is $u(t)=1/2 t \sin(t)$, which clearly grows over time. In applying perturbation theory, the goal is to select the undetermined coefficients in Equation (2-4) to eliminate terms which match the frequency of Equation (2-3). In particular, for the van der Pol equation, the coefficients of any $\sin(t)$ or $\cos(t)$ term must be suppressed when they appear on the right hand sides of Equations (2-6).

As a demonstration, consider the first few orders of ε in Equations (2-6). Starting with zeroeth order, the solution must be of the form:

$$u_0(t) = A_0 \cos(t) + B_0 \sin(t) \tag{2-8}.$$

Now applying the initial condition in Equation (7), $B_0=0$ and A_0 will be determined while solving the first order equation. Substituting $x_0(t)$ into the first order equation and employing trigonometric identities:

$$\begin{aligned}
 u_1'' + u_1 &= (A_0 \cos(t))'(1 - (A_0 \cos(t))^2) - 2\omega_1 (A_0 \cos(t)) \\
 &= \left(-A_0 + \frac{1}{4} A_0^3\right) \sin(t) + \frac{1}{4} A_0^3 \sin(3t) - 2\omega_1 A_0 \cos(t)
 \end{aligned} \tag{2-9}.$$

In order to suppress the secular terms, the coefficients of $\sin(t)$ and $\cos(t)$ must be set equal to zero; there are three possible values for A_0 to do this, $A_0=-2, 0$ or 2 and ω_1 must be zero. Selecting $A_0=0$ will result in the trivial solution for the zeroeth order equation,

but either 2 or -2 would be valid and give solutions to Equation (2-1) with opposite signs. For convenience, take the solution $A_0=2$. The right hand side of Equation (2-9) is now $2 \sin(3t)$ and the solution is:

$$u_1(t) = B_1 \sin(t) - \frac{1}{4} \sin(3t) \quad (2-10)$$

and imposing the initial condition of Equation (2-1) again:

$$u_1(t) = \frac{3}{4} \sin(t) - \frac{1}{4} \sin(3t). \quad (2-11)$$

It serves little point to continue this procedure here, but it is worth noting that both the first order term of the solution, $u_1(t)$, and the first order term in the frequency expansion, ω_1 , were determined from the first order equation of Equations (2-6). This pattern will hold while solving Equations (2-6) at each order of ϵ . Following this procedure, it is possible to find solutions for all $u_i(t)$ and ω_i up to a high value of i ; such a solution is considered an i^{th} order solution to the differential equation [14].

This can be a tedious solution procedure, but the main advantage is that any degree of accuracy can be achieved. In particular, if the solution is needed to some high order n , this method will allow determining the solution of Equation (2-1) through order n with sufficient time and effort. Fortunately, this method (Lindstedt's method) can be realized using a programmable, symbolic algebra package. The results outlined here were determined using a program written in Mathematica™ [9, 32]; the code to generate these results is found in Appendix A. This code takes advantage of some additional features of the van der Pol equation that will be discussed in the next section.

SYMMETRY IN THE VAN DER POL EQUATION

Examining Equation (2-6) with symmetry of the solution in mind, it can be seen that the right hand sides of the equations alternate in symmetry. In particular, the right hand side of the zeroeth order equation is 0 which is even, therefore $u_0(t)$ must be even, which it is. The right hand side of the first order equation, considering the fact that $u_0(t)$ is even, must be odd resulting in an odd solution for $u_1(t)$. This pattern continues and allows the rapid solving of each order of the power series solution.

One additional property of the equation may be used to accelerate the solution of Equations (2-6). Since the left hand side of every order in ϵ is the same, namely:

$$\text{LHS} = u_i'' + u_i \quad (2-12)$$

then the homogeneous solution is always of the form:

$$u_{i,h}(t) = A_i \cos(t) + B_i \sin(t) \quad (2-13)$$

and due to the argument of the above paragraph, $A_i=0$ if i is odd or $B_i=0$ if i is even.

Even more fortunately, the particular solution for each order in ϵ is also predictable. The right hand side of Equation(2-6), after suppressing secularity, will always take the form of:

$$\begin{aligned} \text{RHS} &= a_0 + \sum_{k=3}^{(2i+1),\Delta=2} a_k \cos(k t) \quad \forall i \in \text{Even} \\ \text{RHS} &= \sum_{k=3}^{(2i+1),\Delta=2} b_k \sin(k t) \quad \forall i \in \text{Odd} \end{aligned} \quad (2-14)$$

This results in particular solutions of the form:

$$\begin{aligned} x_{i,p}(\tau) &= \sum_{k=3}^{(2i+1),\Delta=2} \frac{a_k}{k^2 - 1} \cos(k t) \quad \forall i \in \text{Even} \\ x_{i,p}(\tau) &= \sum_{k=3}^{(2i+1),\Delta=2} \frac{b_k}{k^2 - 1} \sin(k t) \quad \forall i \in \text{Odd} \end{aligned} \quad (2-15)$$

The overall advantage of being able to write down these solutions, is that Lindstedt's method may now be used without actually solving any differential equations. This significantly speeds up the solution generation for the van der Pol equation.

After removing the need for using a differential equation solver, the next most time-intensive process left in solving each order of the van der Pol equation is expanding the right hand side of each equation and using the trigonometric identities to reduce them to the form of Equation (2-14). One very simple way to reduce the computational effort is to use Euler's identity:

$$\begin{aligned} e^{jt} &= \cos(t) + j \sin(t), \text{ or} \\ \cos(t) &= \frac{e^{jt} + e^{-jt}}{2} \quad \text{and} \quad \sin(t) = \frac{e^{jt} - e^{-jt}}{2j} \end{aligned} \quad (2-16)$$

where $j = \sqrt{-1}$. Further, in using MathematicaTM, the expression $\text{Exp}(j t)$ is very complicated, so it is advantageous to define another symbol, say $Z \equiv \text{Exp}(j t)$, and then replace each sine and cosine term on the right hand side of Equations (2-6) with:

$$\text{Cos}(kt) = \frac{Z^k + Z^{-k}}{2} \quad \text{and} \quad \text{Sin}(kt) = \frac{Z^k - Z^{-k}}{2j} \quad (2-17)$$

Using these expressions, the right hand side equations can be expanded much more rapidly and then regrouped back into terms of sines and cosines to implement Equation (2-15) and suppress secularity.

The first few terms of the solution of Equation (2-1) are presented here:

$$\begin{aligned} u(t) = & 2 \text{Cos}(t) + \\ & \epsilon \left(\frac{3 \text{Sin}(t)}{4} - \frac{1}{4} \text{Sin}(3t) \right) + \epsilon^2 \left(-\frac{\text{Cos}(t)}{8} + \frac{3}{16} \text{Cos}(3t) - \frac{5}{96} \text{Cos}(5t) \right) + \\ & \epsilon^3 \left(-\frac{7 \text{Sin}(t)}{256} + \frac{21}{256} \text{Sin}(3t) - \frac{35}{576} \text{Sin}(5t) + \frac{7}{576} \text{Sin}(7t) \right) + O(\epsilon^4) \end{aligned} \quad (2-18)$$

with the frequency expansion given by:

$$\omega = 1 - \frac{\epsilon^2}{16} + \frac{17\epsilon^4}{3072} + \frac{35\epsilon^6}{884736} - \frac{678899\epsilon^8}{5096079360} + \frac{28160413\epsilon^{10}}{2293235712000} + O(\epsilon^{12}) \quad (2-19)$$

Using the short-cuts listed above, the code found in Appendix A was developed. The first ten terms in the solution of the van der Pol equation are found in Appendix C along with numerical solutions up through order 25. The solution to the van der Pol equation was determined analytically (no numerical rounding) up through order 75 using this code.

CHAPTER 3: BRIEF DESCRIPTION OF PADÉ APPROXIMANTS

WHAT IS A PADÉ APPROXIMANT?

A Padé approximant is a rational function which approximates a power series [12,13]. It is represented by $[L/P]$ where the numerator is of degree L and the denominator is of degree P. The Padé approximant $[L/P]$ can be constructed from any power series of degree N:

$$f(z) = \sum_{i=0}^{\infty} c_i z^i = c_0 + c_1 z + c_2 z^2 + \dots + c_N z^N + O(z^{N+1}) \quad (3-1)$$

where $L + P \leq N$, and takes the form:

$$[L / P] = \frac{a_0 + a_1 z + a_2 z^2 + \dots + a_L z^L}{b_0 + b_1 z + b_2 z^2 + \dots + b_P z^P} + O(z^{L+P+1}) \quad (3-2)$$

and the Padé approximant's Maclaurin series expansion must match Equation (3-1) exactly up through order $L + P$. In order to make $[L/P]$ unique (since multiplying the numerator and denominator by any value would create another approximant with the same Maclaurin series), it is common to arbitrarily set $b_0=1$ (or divide both the numerator and denominator by b_0), thus making Equation (3-2):

$$[L / P] = \frac{a_0 + a_1 z + a_2 z^2 + \dots + a_L z^L}{1 + b_1 z + b_2 z^2 + \dots + b_P z^P} + O(z^{L+P+1}) \quad (3-3)$$

Note: The power series of Equation (3-1) is assumed to be complex-valued and could represent a Maclaurin series expansion of some function $f(z)$; however, the power series need not be complex-valued in order to work with Padé approximants and Equation (3-1) could just as easily represent the Taylor's series expansion of a real valued function, or an experimentally obtained polynomial curve fit, or a power series solution obtained with perturbation theory.

WHAT ARE PADÉ APPROXIMANTS FOR?

There are three main reasons for constructing Padé approximants.

The first reason to construct [L/P] is to produce a function which has a larger radius of convergence than the original power series. In some cases [L/P] may have a significantly larger radius of convergence than the original power series, or possibly even converge for all values of z . Even if the approximant does not have a larger radius of convergence, the approximant may yield information about how the function behaves for large values of z . This will be more readily seen in an example.

EXAMPLE 3-1

Consider a power series:

$$f(x) = 1 - x + x^2 - x^3 + \dots$$

which is the Taylor's series for $1/(1+x)$ has a radius of convergence $R < 1$. But the an approximant for $f(x)$ is given by

$$[1/1] = \frac{1}{1+x}$$

which is the original function and is finite for all x except $x=-1$ and converges for $R < \infty$. One can see the behavior of $f(x)$ and $[1/1]$ easily in a graph ($f(x)$ is the dotted line, $[1/1]$ is solid) where $f(x)$ includes the first 8 terms in the series:

$f(x)$ & $[1/1]$

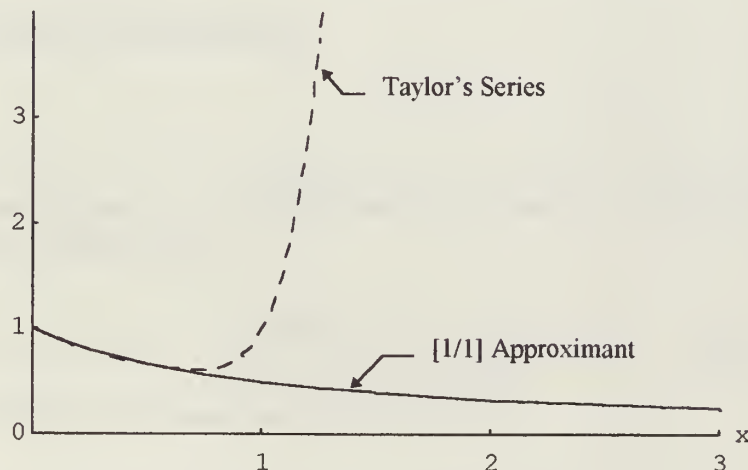


Figure (3-1) Taylor's series and Padé approximant for $1/(1+x)$.

Here, the approximant obviously does a better job of estimating the function for $x > 1$, since the approximate is exactly the same as the original function.

The second reason for using Padé approximants is to speed up the evaluation of a given power series when working inside the radius of convergence. For the preceding example, it is less computationally expensive to find the value of $1+x$ and its reciprocal than it is to evaluate the Taylor's series. In a more general sense, comparing the evaluation of two polynomials of degree $N/2$ and taking their ratio is a less costly evaluation than calculating the value of an N degree polynomial, due to the expense of calculating higher powers in the N degree polynomial.

The third reason for employing Padé approximants, which is closely related to the first, is to more accurately model the asymptotic behavior of a function. One of the worst features about a power series solution is that the highest order term will always dominate when x is large, so the series behaves as x^N . This may be unfortunate, especially if there is some indication of how the actual solution should behave. For example, if the function being modeled is known to decay as $1/x$ or is known to approach a constant value, then a Padé approximant should be more successful in predicting the asymptotic behavior by careful selection of L and P when constructing the $[L/P]$ approximant. In the case of a function which should decay as $1/x$, selecting $P=L+1$ will probably result in an approximant that also behaves as $1/x$ in the limit as x becomes large since the numerator will behave as x^L and the denominator as x^{L+1} . In the case where the function should approach a constant, picking $L=P$ will most likely produce an approximant with the desired behavior. (Example 3 below will explore some of this more clearly.)

CALCULATING PADÉ APPROXIMANTS

PROCEDURE

Calculating a Padé approximant is a straight-forward process [13]. Starting by setting Equation (3-1) equal to Equation (3-3):

$$c_0 + c_1 z + c_2 z^2 + \dots + c_N z^N = \frac{a_0 + a_1 z + a_2 z^2 + \dots + a_L z^L}{1 + b_1 z + b_2 z^2 + \dots + b_P z^P} \quad (3-4)$$

Next, multiply both sides by the denominator of the right side:

$$(c_0 + c_1 z + c_2 z^2 + \dots + c_N z^N)(1 + b_1 z + b_2 z^2 + \dots + b_P z^P) = a_0 + a_1 z + a_2 z^2 + \dots + a_L z^L \quad (3-5)$$

Multiplying Equation (3-5) out and collecting like powers of z , yields:

$$\begin{bmatrix} c_{L-P+1} & c_{L-P+2} & \cdots & c_L \\ c_{L-P+2} & c_{L-P+3} & \cdots & c_{L+1} \\ \vdots & \vdots & \ddots & \vdots \\ c_L & c_{L-P+1} & \cdots & c_{L+P-1} \end{bmatrix} \begin{bmatrix} b_P \\ b_{P-1} \\ \vdots \\ b_1 \end{bmatrix} = - \begin{bmatrix} c_{L+1} \\ c_{L+2} \\ \vdots \\ c_{L+P} \end{bmatrix} \quad (3-6)$$

where $c_j = 0$ if $j < 0$ for consistency, and

$$\begin{aligned} a_0 &= c_0 \\ a_1 &= c_1 + b_1 c_0 \\ a_2 &= c_2 + b_1 c_1 + b_2 c_0 \\ &\vdots \\ a_L &= c_L + \sum_{i=1}^{\min(L,P)} b_i c_{L-i} \end{aligned} \quad (3-7).$$

The linear system in Equation (3-6) may be solved for the b_i 's by any suitable method, and then the b_i 's used in Equations (3-7) to find the a_i 's. Following this procedure, any order Padé approximant can be constructed for $L + P \leq N$.

Equations (3-6) and (3-7) can be easily coded into any programming language or written as functions in many mathematics packages.

EXAMPLES

EXAMPLE 3-2

Find [4/4] for the Taylor's series approximation to $\sin(x)$. Starting with the Taylor's series:

$$f(x) = x - \frac{x^3}{3!} + \frac{x^5}{5!} - \frac{x^7}{7!} + O(x^9)$$

and [4/4] is

$$[4/4] = \frac{a_0 + a_1 x + a_2 x^2 + a_3 x^3 + a_4 x^4}{1 + b_1 x + b_2 x^2 + b_3 x^3 + b_4 x^4}$$

Using Equation (3-6):

$$\begin{bmatrix} 1 & 0 & -1/3! & 0 \\ 0 & -1/3! & 0 & 1/5! \\ -1/3! & 0 & 1/5! & 0 \\ 0 & 1/5! & 0 & -1/7! \end{bmatrix} \begin{bmatrix} b_4 \\ b_3 \\ b_2 \\ b_1 \end{bmatrix} = -\begin{bmatrix} 1/5! \\ 0 \\ -1/7! \\ 0 \end{bmatrix} \Rightarrow \begin{bmatrix} b_4 \\ b_3 \\ b_2 \\ b_1 \end{bmatrix} = \begin{bmatrix} 11/5880 \\ 0 \\ 3/49 \\ 0 \end{bmatrix}$$

$$a_0 = 0$$

$$a_1 = 1 + 0 = 1$$

$$a_2 = 0 + 0 + 0 = 0$$

$$a_3 = -1/6 + 0 + 3/49 + 0 = -31/294$$

$$a_4 = 0 + 0 + 0 + 0 + 0 = 0$$

so the final solution is:

$$[4/4] = \frac{x - \frac{31}{294}x^3}{1 + \frac{3}{49}x^2 + \frac{11}{5880}x^4} + O(x^9).$$

Note: Padé approximants do not perform much better than regular power series in predicting periodic functions; this example was included for numerical interest as will be discussed later.

EXAMPLE 3-3

Another example of finding a Padé approximant demonstrates how asymptotic behavior for Padé approximants may be significantly better than a normal power series. Consider the function:

$$f(x) = \frac{1}{\sqrt{1+x^2}} \text{ with Padé approximant } [3/4] = \frac{1 + \frac{1}{2}x^2}{1 + x^2 + \frac{1}{8}x^4}.$$

Selecting a [3/4] approximant increases the likelihood of correctly modeling the $1/x$ behavior of $f(x)$ for large x . Attempting to calculate the [3/4] approximant yields a [2/4] approximant which shows that not all degree approximants are necessarily unique. Below is a graph of $f(x)$ (solid

line), [3/4] (dotted line) and the eighth order Taylor's series for $f(x)$ (dash-dot). In this case, the [3/4] approximant does a significantly better job of modeling the original equation and tends to zero (as $1/x^2$) for large x .

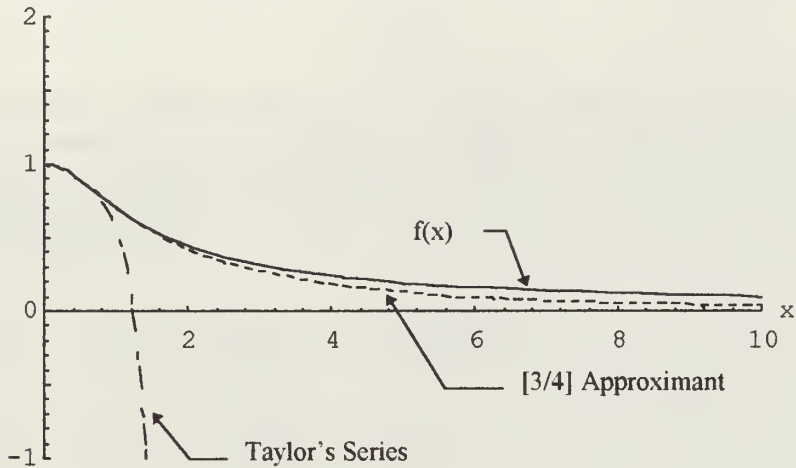


Figure (3-2) Taylor's series and a [3/4] approximant to $f(x) = \frac{1}{\sqrt{1+x^2}}$.

STABILITY OF PADÉ APPROXIMANTS

CONDITION NUMBER CONSIDERATIONS

Following the procedure set out here for finding a Padé approximant includes solving the linear system represented by Equation (3-7) and Equations (3-7). While Equations (3-7) present no difficulties computationally, the solution to Equation (3-6) may be subject to significant loss of numerical accuracy. This is of particular concern when combined with the fact that the accuracy of Padé approximants is highly sensitive to the differences between coefficients in the approximant. (The need for very high numerical accuracy is discussed in detail in Reference [13], section 2.1.)

To illustrate how significant the numerical results may be affected when solving Equation (3-6), one can examine the condition number (or a reasonable approximation for the condition number) of the matrix C :

$$C = \begin{bmatrix} c_{L-P+1} & c_{L-P+2} & \cdots & c_L \\ c_{L-P+2} & c_{L-P+3} & \cdots & c_{L+1} \\ \vdots & \vdots & \ddots & \vdots \\ c_L & c_{L+P+1} & \cdots & c_{L+P-1} \end{bmatrix} \quad (3-8).$$

To gain some measure of the magnitude of the condition number of this matrix, consider the calculations carried out in Example 3-2. Below is a table which shows how the condition number of C varies with the degree of the Padé approximant used to estimate the function $f(x) = \text{Sin}(x)$ and the number of lost digits in accuracy is assumed to be $\text{Log}_{10}(\text{condition number})$:

L=P	Cond #	Lost Digits
4	$4.72 \cdot 10^4$	4
5	$1.66 \cdot 10^5$	5
6	$4.27 \cdot 10^7$	8
7	$3.40 \cdot 10^9$	10
8	$1.74 \cdot 10^{12}$	12
9	$2.46 \cdot 10^{14}$	14
10	$2.08 \cdot 10^{17}$	17

Table (3-1) Condition number and loss of accuracy for Example (3-2).

The importance of finding an accurate method to solve Equation (3-6) is apparent with respect to these results, and it would be wise to check the condition number of C when employing Padé approximants.

There is one obvious way to avoid the numerical problems discussed here. By employing one of the powerful math packages available which can do exact arithmetic such as Mathematica™ or Maple™, Equation (3-6) can be solved with no loss of accuracy when the coefficients c_j are known as precise fractions. While it may seem optimistic to want to know the c_j 's exactly, in many applications where Padé approximants are used, the power series being replaced is generated exactly from a technique such as perturbation theory. In particular, in non-linear vibration analysis, the solution to a differential equation may be a power series in the non-linear parameter, ϵ , known to 50 or even 100 terms which are calculated with fractions and known precisely. This will be discussed more fully when examining applications of Padé approximants to vibration analysis.

What is a defect?

In simple terms, a defect is a failure of a Padé approximant to accurately approximate a power series in the neighborhood of a root of the denominator of the approximant. Or in mathematical terms, a defect occurs around $x=x_D$ when $1+b_1x_D+b_2x_D^2+\cdots+b_Px_D^P=0$. Borrowing on the language of complex analysis, the defect occurs where $[L/P]$ has a pole at x_D or z_D .

How to handle a defect

The presence of the pole in $[L/P]$ may or may not be a result of numerical inaccuracy in calculating the approximant, and on a first look it seems reasonable that there would be cases where we would expect the poles to be present. The most obvious reason for the $[L/P]$ approximant to have a pole would be if the original function, $f(z)$, also has a pole. In this case, the behavior of the approximant will depend on the nature of the pole in $f(z)$; if the pole is an essential pole (there is no finite n such that $(z-z_D)^n f(z)$ is analytic at z_D) then the approximant will always have a defect at z_D , regardless of the degree of $[L/P]$. However, if the pole in $f(z)$ is pole of finite order, it may be possible to remove the defect in the approximant by constructing $[L/P]$ with L and P large enough. There is no guarantee that such an approximant is possible to construct, but taking higher degree approximants frequently removes defects when applied to perturbation theory.

A defect may also occur in an approximant when $f(z)$ has no poles. In this case, the defect could occur due to computational errors which can be significant as discussed in the last section. To handle defects of this nature, there are two basic approaches. One approach is to use a more accurate method to compute the solution of Equation (3-6). This may entail finding the coefficients in the original power series to greater accuracy, using a machine capable of higher accuracy or resorting to rational approximants of the coefficients of the original power series and then solving Equation (3-6) exactly. The second method would be to try calculating the approximant to *lower* degree in the hopes that the C matrix condition number will be enough smaller to prevent the resulting approximant from having a defect.

Another cause for a defect to occur is trying to approximate a complicated function by too low an order Padé approximant. If this is the case, merely finding a higher order approximant will remove the defect with little effort. Coupling this comment with the last point in the previous paragraph, it seems that trying various degree approximants (higher and lower) until finding one that is defect-free is a reasonable approach; however, checking the condition number of C is an intelligent starting point to determine if the difficulty is computational.

More information on making the calculation of Padé approximants numerically stable can be found in Reference [13].

APPLYING PADÉ APPROXIMANTS TO PERTURBATION RESULTS

Having briefly explored one type of perturbation theory application, there are some obvious opportunities to apply Padé approximants to good ends.

One of the most direct applications for Padé approximants in vibrations is to predict the frequency response of a system in terms of the non-linearity parameter ϵ . There are many different methods for estimating the natural frequency of slightly non-linear systems ($\epsilon \ll 1$), but many are inaccurate if the system is tuned such that ϵ is slightly larger. Given that, it is reasonable to calculate a Padé approximant for the frequency of a non-linear system obtained with a perturbation technique in an effort to accurately predict the response frequency for larger ϵ . As a starting point, it is assured that a straight power series for ω will fail to accurately predict the frequency an oscillatory solution as ϵ increases except in very special circumstances. In the general case the frequency will not grow as ϵ^n which is the asymptotic behavior of the power series for large ϵ . This can be seen by examining the power series expansion for the frequency of the van der Pol equation.

EXAMPLE 3-4

Returning to the van der Pol oscillator, Equation (1-1), and using Lindstedt's method, the frequency can be found to high order in ϵ . (This result was derived in Chapter 2.) The first few terms are:

$$\omega = 1 - \frac{1}{16}\epsilon^2 + \frac{17}{3072}\epsilon^4 + \frac{35}{884736}\epsilon^6 - \frac{678899}{5096079360}\epsilon^8 + O(\epsilon^{10}).$$

Taking the [4/4] approximant:

$$[4/4] = \frac{1 + \frac{492389}{2698560}\epsilon^2 + \frac{433361}{34541568}\epsilon^4}{1 + \frac{661049}{2698560}\epsilon^2 + \frac{1285087}{57569280}\epsilon^4}$$

Graphing both the power series for ω (dashed) and [4/4] (solid):

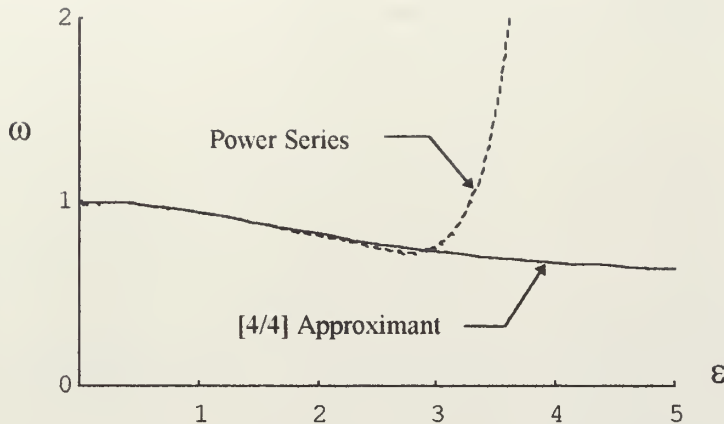


Figure (3-3) Power series and Padé approximant to the frequency of a van der Pol limit cycle.

From experimental data, the van der Pol oscillator is in fact a softening system, meaning the frequency of the response decreases with increased non-linear effects. Also, just from examining the graph, the behavior of the [4/4] approximant seems to continue the pattern of the power series expansion, before ϵ became large enough to make ω start to grow quickly. Both point to the fact that the Padé approximant does a good job of extending the approximation for frequency response as ϵ increases.

LARGE ϵ CONCERNS

Another area where Padé approximants are very useful in vibration theory is in application to relaxation oscillators. Relaxation oscillators have numerous applications in biological systems including how the heart beats, how fish swim (modeling the synapses in the fish's central nervous system), and have possible application as control circuits for robotics. The relaxation oscillator is modeled by a non-linear differential equation where the non-linearity is allowed to become large compared to the linear components in the system, meaning in the neighborhood of 10 or 100 times larger. Consider the relaxation limit for the van der Pol oscillator, Equation (1-1), which behaves as a relaxation for large ϵ . As seen in Example 3-4, the Padé approximant for the frequency more reasonably predicts behavior in the relaxation limit.

APPLICATION TO COUPLED VAN DER POL OSCILLATORS

The main reason for presenting this information on Padé approximants is in applying the theory to the stability transition curves that will be derived in Chapter 5. For the remainder of this thesis, some basic familiarity with Padé approximants will be assumed as they will be used to estimate the frequency of the limit cycle of Equation (1-1), the Zero

Mean Damping Surface described in Chapter 4, and the Stability Transition Curves found in Chapter 5.

CHAPTER 4: COUPLED OSCILLATOR ANALYSIS

PROPOSED MODEL FOR COUPLED OSCILLATORS

As discussed in the introduction, the pair of van der Pol oscillators (x and y) will be modeled by two van der Pol equations coupled with a linear spring and a linear damper. The coupling will be “weak” in the respect that the spring and damper will both be order ϵ ; in particular the stiffness constant will be ϵA and the damping constant will be ϵB where ϵ is the same non-linear parameter as in the original oscillator. The coupled equations take the following form [18]:

$$\begin{aligned}\ddot{x} - \epsilon(1 - x^2)\dot{x} + x &= \epsilon A(y - x) + \epsilon B(\dot{y} - \dot{x}) \\ \ddot{y} - \epsilon(1 - y^2)\dot{y} + y &= \epsilon A(x - y) + \epsilon B(\dot{x} - \dot{y})\end{aligned}\tag{4-1}$$

where dots represent derivatives with respect to time τ .

The object is to determine the existence and stability of solutions to Equation (4-1). In particular, it is desired to find what values for ϵA and ϵB result in orbitally stable solutions.

In this context, orbitally stable is most easily described in the phase plane. Consider the phase plane of the original van der Pol equation plotted in Figure (1-1); the limit cycle presented is orbitally stable. In mathematical parlance, for any small perturbation of the system away from the described limit cycle, there exists a finite distance δ such that the maximum distance between any point on the disturbed path and the original limit cycle is less than or equal to δ [14]. Understanding the concept of orbital stability is essential to comprehending the behavior of coupled oscillators.

By inspection, an exact in-phase motion of the coupled oscillators is possible with $x(\tau) = y(\tau)$. In that case, the coupling terms identically vanish and $x(\tau)$ and $y(\tau)$ will have to satisfy the original van der Pol equation as found in Chapter 1 with $x(\tau) = y(\tau) = u(\tau)$. In this situation, the behavior of each of the coupled oscillators is exactly the same as the original solution, namely each oscillator would exhibit an orbitally stable limit cycle in its own two dimensional phase plane, as seen in Figure (1-1).

In the same vein, it is possible to take advantage of the known properties of $u(\tau)$ by considering $x(\tau)$ and $y(\tau)$ as functions which vary from $u(\tau)$ by small amounts. Treating x and y as variations away from the solution of the van der Pol equation clarifies the meaning of “stability” as applied to the coupled equations of Equation (4-1). While studying the variations away from $u(\tau)$, determining the stability of x and y is equivalent to studying the origin in the variational space. This will be addressed in more detail after deriving the variational equations.

DERIVATION OF THE VARIATIONAL EQUATIONS

Treating $x(\tau)$ and $y(\tau)$ as small variations from $u(\tau)$, the stability of the solutions of Equation (4-1) can be determined by characterizing the behavior of the variations. Consider both functions as small variations from the limit cycle $u(\tau)$ [28]:

$$\begin{aligned}\xi &= x - u & \Rightarrow & \quad x = \xi + u \\ \eta &= y - u & \Rightarrow & \quad y = \eta + u\end{aligned}\tag{4-2}$$

where ξ is the variation of $x(\tau)$ from $u(\tau)$ and η is the variation of $y(\tau)$ from $u(\tau)$. Replacing x and y in Equation (4-1) and rearranging terms yields:

$$\begin{aligned}\ddot{\xi} - \varepsilon(1 - \xi^2 - 2u\xi - u^2)\dot{\xi} + (1 + 2\varepsilon u \dot{u})\xi + \{\ddot{u} - \varepsilon(1 - u^2)\dot{u} + u\} &= \\ \varepsilon A(\eta - \xi) + \varepsilon B(\dot{\eta} - \dot{\xi}) & \\ \ddot{\eta} - \varepsilon(1 - \eta^2 - 2u\eta - u^2)\dot{\eta} + (1 + 2\varepsilon u \dot{u})\eta + \{\ddot{u} - \varepsilon(1 - u^2)\dot{u} + u\} &= \\ \varepsilon A(\xi - \eta) + \varepsilon B(\dot{\xi} - \dot{\eta}) &\end{aligned}\tag{4-3}$$

where the terms in braces are the original van der Pol equation and are identically equal to zero, resulting in:

$$\begin{aligned}\ddot{\xi} - \varepsilon(1 - \xi^2 - 2u\xi - u^2)\dot{\xi} + (1 + 2\varepsilon u \dot{u})\xi &= \varepsilon A(\eta - \xi) + \varepsilon B(\dot{\eta} - \dot{\xi}) \\ \ddot{\eta} - \varepsilon(1 - \eta^2 - 2u\eta - u^2)\dot{\eta} + (1 + 2\varepsilon u \dot{u})\eta &= \varepsilon A(\xi - \eta) + \varepsilon B(\dot{\xi} - \dot{\eta})\end{aligned}\tag{4-4}$$

In the interest of studying only small variations from the limit cycle, non-linear terms in ξ and η are neglected:

$$\begin{aligned}\ddot{\xi} - \epsilon(1-u^2)\dot{\xi} + (1+2\epsilon u \dot{u})\xi &= \epsilon A(\eta - \xi) + \epsilon B(\dot{\eta} - \dot{\xi}) \\ \ddot{\eta} - \epsilon(1-u^2)\dot{\eta} + (1+2\epsilon u \dot{u})\eta &= \epsilon A(\xi - \eta) + \epsilon B(\dot{\xi} - \dot{\eta})\end{aligned}\quad (4-5).$$

In order to simplify the coupling terms appearing on the right hand sides of Equation (4-5), two new equations can be formed by adding and subtracting the two Equations (4-5) and letting:

$$\begin{aligned}\dot{w} &= \xi + \eta \\ \dot{v} &= \xi - \eta\end{aligned}\quad (4-6).$$

So Equations (4-5) become:

$$\begin{aligned}\ddot{w} - \epsilon(1-u^2)\dot{w} + (1+2\epsilon u \dot{u})\dot{w} &= 0 \\ \ddot{v} - \epsilon(1-2B-u^2)\dot{v} + (1+2\epsilon u \dot{u} + 2\epsilon A)\dot{v} &= 0\end{aligned}\quad (4-7).$$

By inspecting Equations (4-7) it can be seen that both equations are exact differentials which can be integrated with respect to time to yield:

$$\begin{aligned}\ddot{w} - \epsilon(1-u^2)\dot{w} + w &= k_1 \\ \ddot{v} - \epsilon(1-2B-u^2)\dot{v} + (1+2\epsilon A)v &= k_2\end{aligned}\quad (4-8).$$

While studying stability, the solutions for $v(\tau)$ and $w(\tau)$ can be recast to further simplify Equation (4-6). The particular solutions to Equations (4-8) are constants, in particular:

$$\begin{aligned}w_p &= k_1 \\ v_p &= \frac{k_2}{1+2\epsilon A}\end{aligned}\quad (4-9).$$

These solutions do not vary with time and can be removed by a simple coordinate transform in the variational space: $w \rightarrow w-w_p$ and $v \rightarrow v-v_p$. Such a transformation will not alter the stability of the solutions, since stability is controlled by the exponential behavior of the functions. Then the varational equations become:

$$\begin{aligned}\ddot{w} - \epsilon(1-u^2)\dot{w} + w &= 0 \\ \ddot{v} - \epsilon(1-2B-u^2)\dot{v} + (1+2\epsilon A)v &= 0\end{aligned}\quad (4-10).$$

In order to study the stability of the coupled van der Pol oscillators, both of Equations (4-10) must be explored and characterized. In order to discover the nature of the first equation in Equation (4-10), consider a small variation from a single van der Pol solution, $u(\tau)$:

$$z(\tau) = u(\tau) + \xi(\tau) \quad (4-11)$$

where $u(t)$ is a solution of the van der Pol equation, Equation (1-1). Substituting z into Equation (1-1) results in:

$$\ddot{u} + \ddot{\xi} + \epsilon \left(1 - (u + \xi)^2 \right) (\dot{u} + \dot{\xi}) + u + \xi = 0 \quad (4-12)$$

which when expanded and eliminating the higher order terms in ξ results in:

$$\left\{ \ddot{u} + \epsilon(1 - u^2) \dot{u} + u \right\} + \ddot{\xi} + \epsilon(1 - u^2) \dot{\xi} + \xi = 0 \quad (4-13)$$

where the term in braces is again the van der Pol equation and is identically zero, resulting in:

$$\ddot{\xi} + \epsilon(1 - u^2) \dot{\xi} + \xi = 0 \quad (4-14).$$

Equation (4-14) is the behavior of a small variation, ξ , away from the orbitally stable van der Pol limit cycle, therefore ξ must be orbitally stable. Comparing Equation (4-14) to the first of Equation (4-10), w and ξ have identical solutions, therefore $w(\tau)$ must be orbitally stable.

Understanding the stability of the first Equation (4-10) leaves only the behavior of the second variational equation:

$$\ddot{v} - \epsilon(1 - 2B - u^2) \dot{v} + (1 + 2\epsilon A)v = 0 \quad (4-15)$$

to be characterized in order to understand the stability of Equations (4-1). Equation (4-15) will be referred to as the variational equation for the remainder of this thesis.

SIGNIFICANCE OF THE ZERO MEAN DAMPING SURFACE

Studying the stability of the variational equation requires characterizing the solutions of Equation (4-15) in the three dimensional parameter space $\{ \epsilon, \epsilon A, \epsilon B \}$. Ultimately, it should be possible to find the surface in $\{ \epsilon, \epsilon A, \epsilon B \}$ space which corresponds to the

transition from stable to unstable oscillations of the coupled equations. Such an analysis is feasible, however it would be formidable to complete using analytical methods. Such an analysis using numerical techniques is underway by Reinhall and Storti[19,20].

In order to reduce the complexity of the problem, the parameter space may be reduced to two dimensions by fixing or specifying any of the three parameters. Such an analysis for the case of $B=0$, i.e. no damping between the coupled oscillators, is presented by Storti and Reinhall [26].

Another obvious two dimensional subspace for studying the variational equation is the Zero Mean Damping (ZMD) surface of the parameter space. The ZMD surface is the locus of values for the damping parameter εB , as a function of ε , resulting in zero time average damping in the variational equation. The ZMD surface is a logical place to study the behavior Equation (4-15) because it marks the boundary between the region of negative mean damping, where all solutions to Equation (4-15) will grow over time due to the energy added by negative damping, from the region where damping is positive on average and stable solutions may be possible. By examining Equation (4-9), the parameter εA does not appear in the damping term, so the ZMD surface will be a function of ε and εB only. The ZMD surface is found by requiring the time average of the coefficient of \dot{v} to vanish in Equation (4-15):

$$\langle 1 - 2B_{ZMD} - u^2 \rangle = 0 \quad (4-16)$$

where the angled brackets indicate time averaging. Clearly B_{ZMD} will be a function of ε since $u(t)$, found in Chapter 1, is a power series in ε .

The balance of this thesis will be dedicated to characterizing the behavior of the variational equation, Equation (4-15), along the ZMD surface.

CALCULATING THE ZMD SURFACE

Performing the time averaging using the solution for $u(t)$ found in Chapter 1 and is a tedious, but straight-forward process. Since B_{ZMD} is not a function of time, Equation (4-16) can be rewritten as:

$$B_{ZMD} = \frac{1}{2} - \frac{1}{2} \langle u^2 \rangle \quad (4-17)$$

Using the solution $u(t)$ generated in Chapter 1, the ZMD surface can be calculated to the same order in ε as $u(t)$. The first few terms of B_{ZMD} are:

$$B_{ZMD} = -\frac{1}{2} - \frac{\epsilon^2}{32} + \frac{11\epsilon^4}{9216} + \frac{4859\epsilon^6}{10616832} - \frac{12921629\epsilon^8}{152882380800} + O(\epsilon^{10}) \quad (4-18).$$

A Padé approximant to the ZMD surface through $O(\epsilon^{20})$ is given by:

$$B_{ZMD} = \frac{-0.5 - 0.185\epsilon^2 - 0.0669\epsilon^4 - 0.0110\epsilon^6 - 0.00132\epsilon^8 - 0.0000589\epsilon^{10}}{1. + 0.307\epsilon^2 + 0.117\epsilon^4 + 0.0163\epsilon^6 + 0.00202\epsilon^8 + 0.0000654\epsilon^{10}} \quad (4-19)$$

where the fractions which actually appear in the Padé approximant have been replaced with 3 decimals of precision. Figure (4-1) is a plot of the Padé approximant [10/10] of B_{ZMD} calculated using exact coefficients.

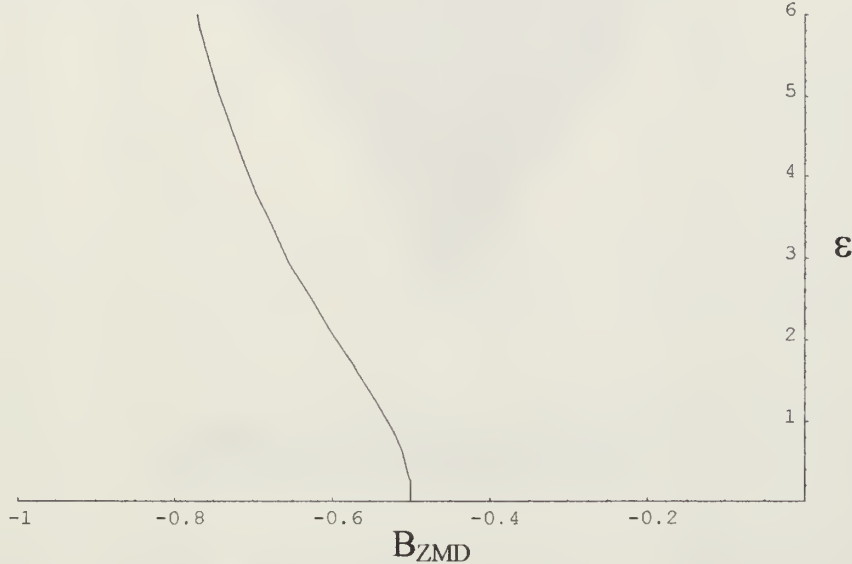


Figure (4-1) Padé approximant to the B_{ZMD} vs. ϵ .

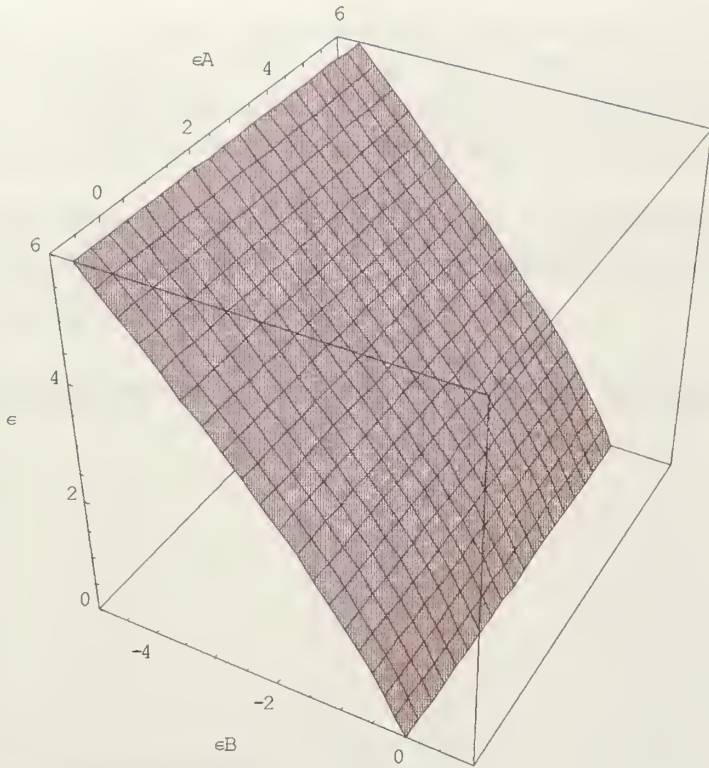


Figure (4-2) Padé approximant to the ZMD surface in 3-D parameter space.

Figure (4-2) shows no additional information from Figure (4-1), but gives a physical feel for the parameter space. The stability transition curves obtained in Chapter 5 should be plotted along this surface in 3-space.

FLOQUET THEORY AND STABILITY TRANSITIONS CURVES

Equation (4-15), the variational equation, is a Hill's equation, meaning it is a linear differential equation with periodic coefficients. This has two important consequences in relation to examining the stability of the solutions of Equations (4-1) along the ZMD surface.

Since Equation (4-15) is a Hill's equation whose periodic coefficients have period π , all stable, periodic solutions will have period π or 2π . Recalling that $u(t)$ is periodic, with period 2π , $u^2(t)$ must have period π ; then the claim follows directly from Floquet's Theorem [16].

The second result of the variational equation being a Hill's equation, is that the transition from stable to unstable behavior in the parameter space will always be through a stable, periodic solution. In combination with the first result, that stable, periodic solution must be of period π or 2π . To prove this claim, consider Floquet's Theorem[14]:

The regular system $\dot{\mathbf{x}} = \mathbf{P}(t)\mathbf{x}$, where \mathbf{P} is an $n \times n$ matrix function with minimal period T , has at least one non-trivial solution $\mathbf{x} = \chi(t)$ such that $\chi(t+T) = \mu \chi(t)$ where μ is a constant.

The variational equation can be written in the form required by Floquet's Theorem by selecting:

$$\mathbf{x} = \begin{Bmatrix} v \\ \dot{v} \end{Bmatrix} \quad (4-20)$$

and identifying:

$$\mathbf{P} = \begin{bmatrix} 0 & 1 \\ -(1+2\varepsilon A) & \varepsilon(1-2B_{ZMD}-u^2) \end{bmatrix} \quad (4-21)$$

which has period π due to the presence of $u^2(t)$. Therefore Equation (4-15) meets the conditions of Floquet's Theorem. Now consider the possible values for μ . If $\mu > 1$ the solution $\chi(t)$ becomes unbounded over time since the solution is multiplied by μ for each interval of time π ; similarly if $\mu < -1$ the solution will also be unbounded over time. In both of these cases the solutions to the variational equation are unstable. If $-1 < \mu < 1$, the solution is stable and decays to the origin over time. That leaves two possible values for μ : $\mu=1$ or $\mu=-1$.

If $\mu=1$, the solution is periodic with period π , the same period as $\mathbf{P}(t)$. If $\mu=-1$, the solution is also periodic but has period 2π . Identifying where the characteristic number, μ , takes on the values of 1 and -1 marks the transition between stable and unstable solutions of the variational equation.

The fact that the transition between stable and unstable behavior is always through a stable, periodic solution with period π or 2π focuses the study of this thesis. Locating the periodic solutions of Equation (4-15) on the ZMD surface identifies the stability transition curves, where the stability transition curves are the curves which divide stable and unstable behavior of Equations (4-1) in the parameter space along the ZMD surface. Hence, the

next task is to identify where periodic solutions (of period π or 2π) of Equation (4-15) exist on the ZMD surface.

CHAPTER 5: PERIODIC SOLUTIONS OF THE VARIATIONAL EQUATION

As discussed at the end of Chapter 4, identifying the periodic solutions of the variational equation along the Zero Mean Damping (ZMD) surface is equivalent to finding the stability transition curves for the coupled oscillators modeled by Equations (4-1). The next task is to find those periodic solutions.

SOLUTION METHOD

The periodic solutions of the variational equation will be identified using Lindstedt's method [14], which was also used in Chapter 1 to solve the van der Pol equation. The variational equation along the zero mean damping surface is restated here for easy referencing:

$$\ddot{v} - \epsilon(1 - 2B - u^2)\dot{v} + (1 + 2\epsilon A)v = 0 \quad (5-1).$$

Some characteristics of the Equation (5-1) are worth mentioning. The most significant feature is that unlike the van der Pol equation itself, the variational equation is a linear ordinary differential equation. Since $u(\tau)$ can be determined to a suitably large order in ϵ as outlined in Chapter 1, and B_{ZMD} is the expansion for the ZMD surface, all the coefficients in the variational equation are known except ϵA . As a consequence of being a linear equation, solutions to Equation (5-1) will also obey the principle of superposition.

Even though Equation (5-1) is a linear differential equation, Lindstedt's method is used to find $v(\tau)$ because of the presence of $u(\tau)$ which is a power series. In keeping with Lindstedt's method, the first step is to rescale time such that $\tau = \omega(\epsilon) t$. Substituting this rescaling into Equation (5-1) and changing the differentiation to the new time scale:

$$v'' - \epsilon(1 - 2B_{ZMD} - u^2)\omega v' + \omega^2(1 + 2\epsilon A)v = 0 \quad (5-2)$$

where primes represent differentiation with respect to the rescaled time t . Notice that here the function $\omega(\epsilon)$ was already determined in solving Equation (1-1) and is given by Equation (1-19). The frequency expansion must be the same as for the original van der Pol solution because the solutions to Equation (5-1) must have the same period or twice the period of its coefficients; this was discussed at the end of Chapter 4. Plugging in power series expansions for ω , v , B_{ZMD} , u and ϵA according to:

$$\begin{aligned}
 \varepsilon A &= A_0 + \sum_{i=1}^n A_i \varepsilon^i \\
 B_{ZMD} &= B_0 + \sum_{i=2}^{n,2} B_i \varepsilon^i \\
 u(t) &= u_0(t) + \sum_{i=1}^n u_i(t) \varepsilon^i \\
 v(t) &= v_0(t) + \sum_{i=1}^n v_i(t) \varepsilon^i \\
 \omega &= 1 + \sum_{i=2}^{n,2} \omega_i \varepsilon^i
 \end{aligned} \tag{5-3}$$

and collecting powers of ε gives a series of linear, ordinary differential equations, the first three of which are presented here:

$$\begin{aligned}
 v''_0 + (1 + 2A_0)v_0 &= 0 \\
 v''_1 + (1 + 2A_0)v_1 &= -2A_1 v_0 + v'_0 - 2B_0 v'_0 - u_0^2 v'_0 \\
 v''_2 + (1 + 2A_0)v_2 &= -2A_2 v_0 - 2A_1 v_1 - 2u_0 u_1 v'_0 + v'_1 - 2B_0 v'_1 - u_0^2 v'_1 - 2\omega_2 u''_0
 \end{aligned} \tag{5-4}.$$

Notice that the left hand side of each of Equations (5-4) is of the same form, namely:

$$\text{LHS} = v''_i + (1 + 2A_0)v_i \tag{5-5}.$$

Insisting that the solution of Equation (5-1) be periodic with period π or 2π , as discussed above, the coefficient for v_i in Equation (5-5) must be an integer squared. This follows directly from the Floquet theory discussed at the end of Chapter 4; the solution to Equation (5-5) is $\cos(t\sqrt{1 - 2A_0})$ which can produce $v(t)$ with period π or 2π only if $\sqrt{1 - 2A_0}$ is an integer; therefore:

$$1 + 2A_0 = k^2 \quad \text{or} \quad A_0 = \frac{k^2 - 1}{2} \quad \text{where} \quad k \in \{1, 2, 3, \dots\} \tag{5-6}.$$

This gives rise to an infinite set of starting values for A_0 , and possible stability transition curves out of each starting value. The first few A_0 's are given here:

$$A_0 = \left\{ -\frac{1}{2}, 0, \frac{3}{2}, 4, \frac{15}{2}, 12, \dots \right\} \tag{5-7}.$$

DEALING WITH $A_0 = -1/2$

When $A_0 = -1/2$, the variational equation changes form significantly; the zeroeth order equation of Equations (5-4) becomes:

$$v_0'' = 0 \quad (5-8)$$

which has solution:

$$v_0 = C_0 + C_{01}t \quad (5-9)$$

However, since the goal is to find periodic, stable solutions to the variational equation, $C_{01} = 0$ so $v_0 = C_0$ is the solution. Plugging in this v_0 and examining the first order equation yields:

$$v_1'' = -2A_1C_0 \quad (5-10).$$

In order for v_1 to be bounded, either $C_0 = 0$ or $A_1 = 0$. The former yields a trivial order zero solution, but the latter is a valid method of solving Equation (5-8) with a bounded solution. By similar arguments used about Equation (5-9) it can be seen that $v_1 = C_1$. Following this pattern, the same equation arises at each order of ϵ , so that the stability transition curve from $A_0 = -1/2$ is in fact just $\epsilon A = -1/2$.

SOLVING FOR THE STABILITY TRANSITION CURVES

For the remainder of the possible values for A_0 listed in Equation (5-7), the solution procedure is a straight-forward application of Lindstedt's method. Whereas the solution of the van der Pol equation in Chapter 1 resulted in fixing the frequency of the response as a function of ϵ , solving the variational equation for $v(t)$ will give the coefficients for the ϵA expansion.

Unfortunately, unlike the arguments made in Chapter 1 for the van der Pol equation, there are no obvious symmetry arguments to use in the solution of the variational equation. While the solution of the variational equation shows interesting patterns for some values of A_0 , the overall pattern is not easily discernible. This results in a very costly computational procedure for determining the stability transition curves.

The stability transition curves calculated below and Tabulated in Appendix E were generated using the Mathematica™ code found in Appendix B. One feature of the code is worth mentioning here. In an effort to make solving the second order differential equations more efficient, a specific solving routine called MySolve[] was written. This

routine takes advantage of the fact that at every order of ϵ , the differential equation encountered always takes the form:

$$v_i'' + k^2 v_i = f(\sin(m t), \cos(m t)) \text{ where } m = 1, 2, 3, \dots, 2i+1 \quad (5-11)$$

and allows the code to produce solutions without calling a general differential equation solver. The specialized solver significantly increases the computational efficiency.

CONDITIONS FOR SUPPRESSING SECULARITY

Following Lindstedt's method and substituting the power series of Equation (5-3) into Equation (5-2) and collecting terms of the same order in ϵ , the first few equations can be obtained:

$$\begin{aligned} k^2 v[0, t] + v^{(0,2)}[0, t] &= 0 \\ k^2 v[1, t] + v^{(0,2)}[1, t] &= -2 a[1] v[0, t] + 2 v^{(0,1)}[0, t] - 4 \cos[t]^2 v^{(0,1)}[0, t] \\ k^2 v[2, t] + v^{(0,2)}[2, t] &= -2 a[2] v[0, t] - 2 a[1] v[1, t] - 3 \cos[t] \sin[t] v^{(0,1)}[0, t] + \\ &\quad \cos[t] \sin[3t] v^{(0,1)}[0, t] + 2 v^{(0,1)}[1, t] - 4 \cos[t]^2 v^{(0,1)}[1, t] + \frac{1}{8} v^{(0,2)}[0, t] \end{aligned} \quad (5-12)$$

where $k^2 = 1 + 2 A_0$ as defined in Equation (5-6). The notation used in Equations (5-12) is consistent with the Mathematica™ code found in Appendix B. In this notation, $v[i, t]$ is the same as $v_i(t)$, $a[i]$ is A_i , and the numbers inside parenthesis represent differentiation with respect to the variable t .

Noting that the left hand side of each of Equations (5-12) are identical, it can be seen that the homogeneous solution for each order of ϵ will be similar:

$$v_h[i, t] = c[i] \cos[k t] + s[i] \sin[k t] \quad (5-13)$$

where $c[i]$ and $s[i]$ will be used consistently to represent the coefficients of the homogeneous solutions of the i^{th} order equation. The particular solutions will not be as consistent, but will be of the form:

$$v_p[i, t] = \sum_{m=0}^{2i+1} \{ c[i, m] \cos[m k t] + s[i, m] \sin[m k t] \} \quad (5-14)$$

The $c[i, m]$ and $s[i, m]$ are tabulated in Appendix D.

In the course of solving Equations (5-11), two unique solutions for suppressing secularity will arise for each A_0 [20]. The outcome of these two possible solutions for $v[t]$ and ϵA is that for each starting value of A_0 , other than $-1/2$, there will be two curves along the ZMD surface which have valid, periodic solutions, with period π or 2π . These curves intersect at $\epsilon A = A_0$ and resemble a horn with its point downward and will sometimes be referred to as the “stability horn” arising from each A_0 . Extending this result into the three dimensional parameter space of Figure (4-2), the two dimensional surface where periodic solutions to Equation (5-2) exist will resemble cones with their points coming out of each A_0 . The regions within the cones are unstable, that is the solutions to the variational equation will grow over time, making the origin of the variational space an unstable equilibrium point. The regions outside of the cones and above the ZMD surface will be asymptotically stable; all solutions will decay towards the origin of the variational space over time. The actual surfaces of the cones are configurations which yield orbitally stable solutions.

One of the main difficulties in solving Equations (5-12) will be to identify this split in the stability conditions. The conditions are different for each A_0 and will be considered one at a time.

CASE 1: $A_0 = 0$

For the case of $A_0 = 0$, Equation (5-6) yields $k=1$. Solving Equations (5-12) and suppressing the secular terms appearing on the right hand side of the first order term gives:

$$\begin{aligned} -c[0] - 2a[1]s[0] &= 0 \\ -2a[1]c[0] - s[0] &= 0 \end{aligned} \tag{5-15}$$

which has two possible solutions for $a[1]$ and $s[0]$:

$$\left\{ \begin{aligned} s[0] &\rightarrow -c[0], a[1] \rightarrow \frac{1}{2} \\ s[0] &\rightarrow c[0], a[1] \rightarrow -\frac{1}{2} \end{aligned} \right\} \tag{5-16}.$$

The first solution will yield a curve to the right of the second when viewed on the ZMD surface. From this point on, the solutions for $v[t]$ and ϵA are unique and the stability transition curves are given by:

$$\begin{aligned} \epsilon A_{\text{low}} &= -\frac{\epsilon}{2} + \frac{\epsilon^2}{8} + \frac{\epsilon^3}{32} - \frac{7\epsilon^4}{384} + \frac{3\epsilon^5}{1024} - \frac{247\epsilon^6}{442368} - \frac{11657\epsilon^7}{21233664} + \frac{1224811\epsilon^8}{2548039680} + O(\epsilon^9) \\ \epsilon A_{\text{up}} &= \frac{\epsilon}{2} + \frac{\epsilon^2}{8} - \frac{\epsilon^3}{32} - \frac{7\epsilon^4}{384} - \frac{3\epsilon^5}{1024} - \frac{247\epsilon^6}{442368} + \frac{11657\epsilon^7}{21233664} + \frac{1224811\epsilon^8}{2548039680} + O(\epsilon^9) \end{aligned} \tag{5-17}.$$

The power series given by Equation (5-17) were calculated out to $O(\epsilon^{33})$ and converted into Padé approximants which are plotted in Figure (5-1) with the power series.

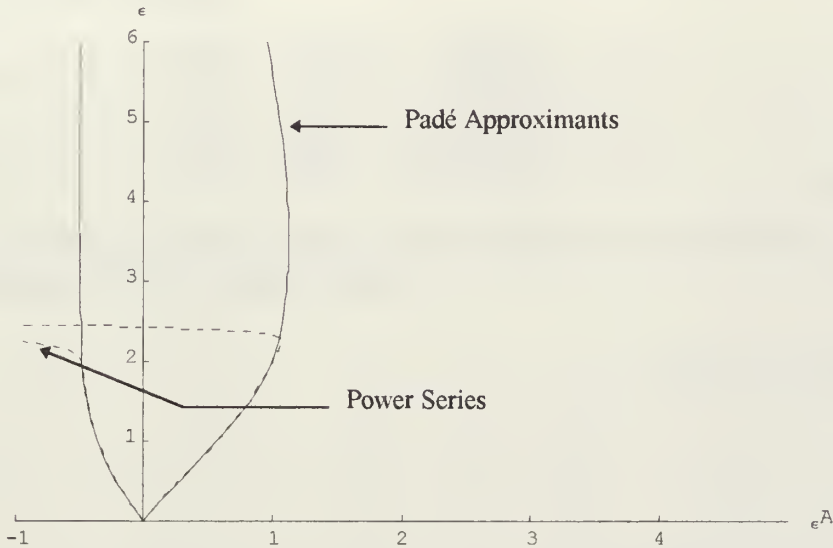


Figure (5-1) Power series and Padé approximants
[16/16] to transition curves out of $A_0=0$.

CASE 2: $A_0 = 3/2$

For $A_0 = 3/2$, Equation (5-6) gives $k=2$. Suppressing the secular terms in the first order equation of Equation (5-12) yields:

$$\begin{aligned} -2 a[1] s[0] &= 0 \\ -2 a[1] c[0] &= 0 \end{aligned} \quad (5-18)$$

which requires $a[1]=0$ for a non-trivial solution. Suppressing secularity in the second order equation:

$$\begin{aligned} \frac{2 s[0]}{3} - 2 a[2] s[0] &= 0 \\ -\frac{c[0]}{3} - 2 a[2] c[0] &= 0 \end{aligned} \quad (5-19)$$

which has three possible solutions:

$$\left\{ \left\{ a[2] \rightarrow -\frac{1}{6}, s[0] \rightarrow 0 \right\}, \left\{ a[2] \rightarrow \frac{1}{3}, c[0] \rightarrow 0 \right\}, \left\{ s[0] \rightarrow 0, c[0] \rightarrow 0 \right\} \right\} \quad (5-20).$$

The last solution is the trivial solution, but the first two again provide the split for the lower and upper stability curves. From this point, the solutions are unique and the stability transition curves are given by:

$$\begin{aligned}\epsilon A_{\text{low}} &= \frac{3}{2} - \frac{\epsilon^2}{6} + \frac{109 \epsilon^4}{3456} - \frac{3419 \epsilon^6}{1990656} - \frac{297305 \epsilon^8}{573308928} + O(\epsilon^{10}) \\ \epsilon A_{\text{up}} &= \frac{3}{2} + \frac{\epsilon^2}{3} - \frac{53 \epsilon^4}{3456} - \frac{6983 \epsilon^6}{1990656} + \frac{740213 \epsilon^8}{2866544640} + O(\epsilon^{10})\end{aligned}\quad (5-21).$$

The Padé approximants for the power series of Equations (5-21) calculated to $O(\epsilon^{33})$ are plotted in Figure (5-2) with the power series.

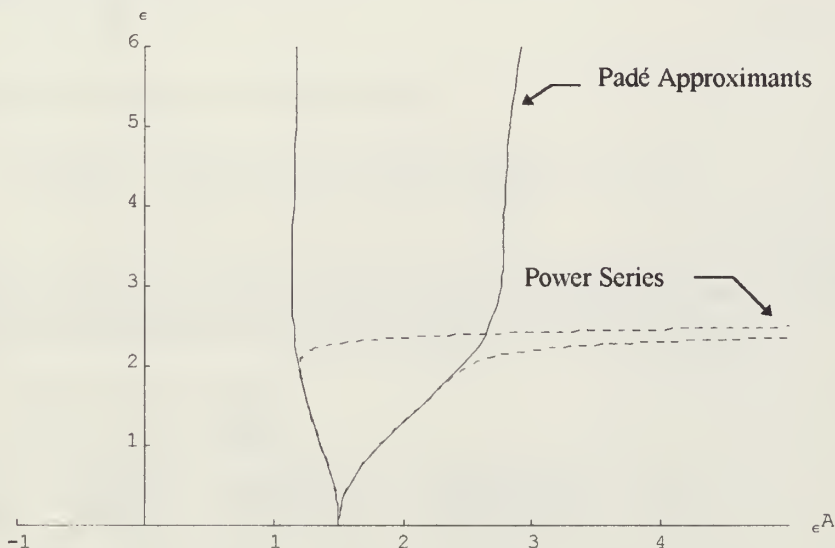


Figure (5-2) Power series and Padé approximants [12/12] to transition curves out of $A_0=3/2$.

CASE 3: $A_0 = 4$

For $A_0 = 4$, Equation (5-6) gives $k=3$. Suppressing the secular terms in the first order equation of Equation (5-12) yields:

$$\begin{aligned}-2 a[1] s[0] &= 0 \\ -2 a[1] c[0] &= 0\end{aligned}\quad (5-22)$$

which requires $a[1]=0$ for a non-trivial solution. Suppressing secularity in the second order equation:

$$\begin{aligned} -\frac{9 s[0]}{16} - 2 a[2] s[0] &= 0 \\ -\frac{9 c[0]}{16} - 2 a[2] c[0] &= 0 \end{aligned} \quad (5-23)$$

which requires $a[2]=-9/32$ for a non-trivial solution. Suppressing secularity in the third order equation:

$$\begin{aligned} \frac{5 c[0]}{32} - 2 a[3] s[0] &= 0 \\ -2 a[3] c[0] + \frac{5 s[0]}{32} &= 0 \end{aligned} \quad (5-24)$$

which has two possible solutions for $a[3]$ and $s[0]$:

$$\left\{ \left\{ s[0] \rightarrow -c[0], a[3] \rightarrow -\frac{5}{64} \right\}, \left\{ s[0] \rightarrow c[0], a[3] \rightarrow \frac{5}{64} \right\} \right\} \quad (5-25).$$

These two solutions provide the split for the lower and upper stability curves. From this point, the solutions are unique and the stability transition curves are given by:

$$\begin{aligned} \epsilon A_{\text{low}} &= 4 - \frac{9 \epsilon^2}{32} - \frac{5 \epsilon^3}{64} + \frac{2877 \epsilon^4}{40960} + \\ &\quad \frac{2537 \epsilon^5}{737280} - \frac{54707 \epsilon^6}{15728640} + \frac{11663959 \epsilon^7}{14155776000} - \frac{17260922723 \epsilon^8}{12683575296000} + O(\epsilon^9) \\ \epsilon A_{\text{up}} &= 4 - \frac{9 \epsilon^2}{32} + \frac{5 \epsilon^3}{64} + \frac{2877 \epsilon^4}{40960} - \frac{2537 \epsilon^5}{737280} - \frac{54707 \epsilon^6}{15728640} - \frac{11663959 \epsilon^7}{14155776000} - \\ &\quad \frac{17260922723 \epsilon^8}{12683575296000} + O(\epsilon^9) \end{aligned} \quad (5-26)$$

The Padé approximants for the power series of Equations (5-26) calculated to $O(\epsilon^{33})$ are plotted in Figure (5-3) with the power series.

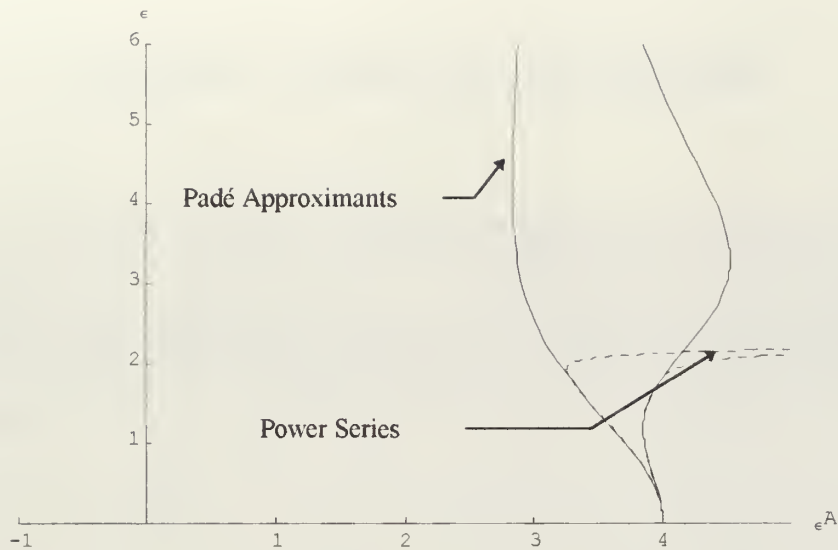


Figure (5-3) Power series and Padé approximants [16/16] to transition curves out of $A_0=4$.

CHAPTER 6: SUMMARY AND FUTURE WORK

In Chapter 5, the first three pairs of stability transition curves along the Zero Mean Damping (ZMD) surface were determined. Combining Figures (5-1,2 and 3) yields the stability regions for the smaller values of εA . In Figure (6-1), U marks regions that are unstable and S marks regions where orbitally stable solutions to the variational equation, Equation (4-15), exist. The stability transition curves are approximated by Padé approximants.

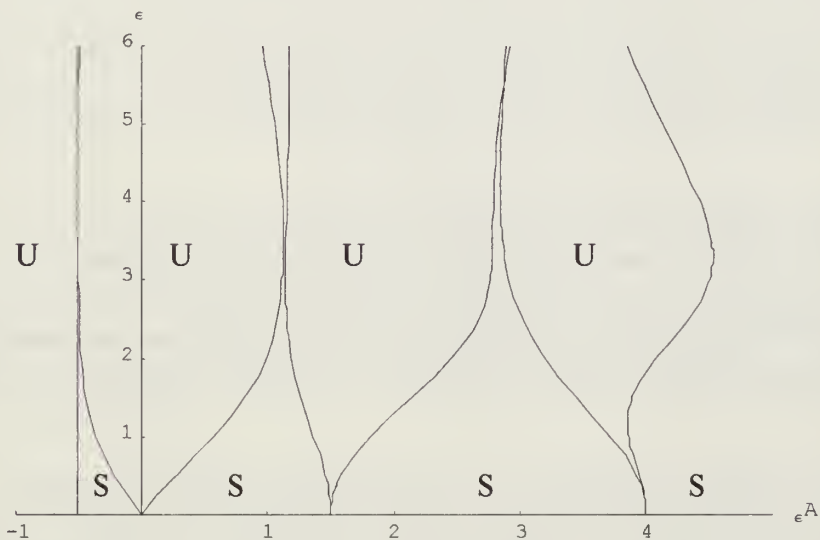


Figure (6-1) Stability regions for coupled VDP oscillators on the ZMD surface.

The three dimensional version of the same graph is given in Figure (6-2) where the three dimensions are the three parameters of Equation (4-1), $\{\varepsilon, \varepsilon A, \varepsilon B\}$. This is a graph of the stability transition curves found in Chapter 5 plotted on the ZMD surface of Figure (4-2).

SUMMARY

Using the techniques outlined in Chapter 5 and employing a symbolic mathematics package (MathematicaTM) the first three pairs of stability transition curves for a pair of weakly coupled van der Pol oscillators were determined. All calculations were carried out exactly, that is exact fractions were used in all computations with no numerical roundoff. Using this analytical approach, the six stability transition curves seen in Figures (6-2) and

(6-2) were calculated to $O(\epsilon^{33})$. The power series coefficients for the transition curves are tabulated in Appendix E.

FUTURE WORK

There are three main areas for future work on this project.

The first is to extend the range of ϵA covered in this thesis, namely find the stability transition curves coming from the rest of the A_0 values given in Equation (5-7). Work on this area, using the code written for this thesis, is already in progress. The main difficulty in finding the stability transition curves coming from the next few values of A_0 is showing that the curves are unique. Present conjecture is that there are more conditions needed to fully specify the upper curves than used in Chapter 5. To find what those conditions might be, research is underway to use Hill's determinants to find the periodic solutions rather than Lindstedt's method.

Another area for future work was hinted at in Chapter 4 when the ZMD surface was introduced. The full challenge for this type of stability analysis would be to find the stability transition surfaces in the three dimensional parameter space. Currently, numerical calculations of this project are under way by Storti and Reinhall (REFERENCE>>>). The logical extension of this project would be to find the transition surfaces analytically to avoid numerical roundoff errors.

The final, and ultimate continuation of this work is to physically realize the coupled relaxation oscillators modeled by Equation (4-1). Once these oscillators are accurately predicted by the mathematical models, they could be used to generate control signals for ambulatory robots, mechanical fish or similar mechanisms. The goal of this thesis was to further understanding toward reaching this goal.

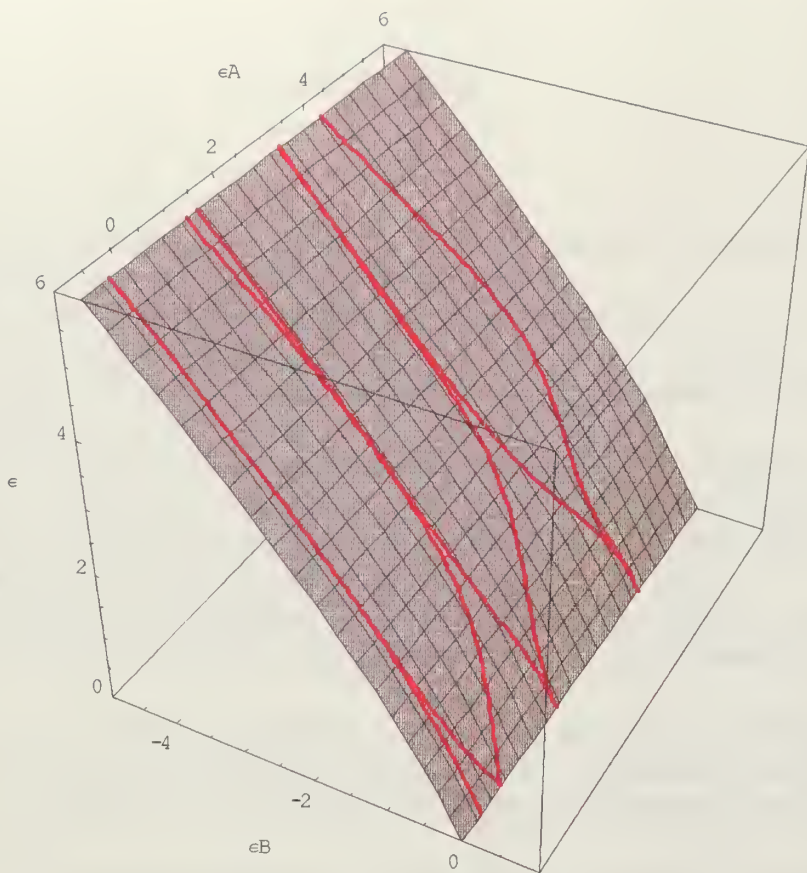


Figure (6-2) Three dimensional plot of the stability transition curves along the ZMD surface.

BIBLIOGRAPHY

1. Andersen, C. M., and Geer, J. F., 1982, *Power Series Expansions for the Frequency and Period of the Limit Cycle of the van der Pol Equation*.
2. Andronov, A.A. and Chaikin, C. E. 1949, *Theory of Oscillations*.
3. Blevins, R.D. 1977, *Flow-Induced Vibration*.
4. Carrier, G.F. 1953, Boundary Layer Problems in Applied Mechanics, *Advances in Applied Mechanics*, 3 , 1-20.
5. Chen, S.-S., 1987, *Flow-Induced Vibration of Circular Cylindrical Structures*.
6. Cohen, A. H. , Holmes, P.J., and Rand, R.H., 1982, The Nature of the Coupling Between Segmental Oscillators of the Lamprey Spinal Generator for Locomotion: A Mathematical Model, *Journal of Mathematical Biology*, 12, 345-369.
7. Dadfar, M.B., Geer, J. and Andersen, C.M., 1984, Perturbation Analysis of the Limit Cycle of the van der Pol Equation, *SIAM Journal on Applied Mathematics*, 44, 881-895.
8. Dorodnitsyn, A.A., 1947, Asymptotic Solution of the van der Pol Equation, *Proceedings of the Institute of Mechanics of the Academy of Science of the USSR*, XI.
9. Gaylord, R. J., Kamin, S. N., and Wellin, P.R., 1993, *Introduction to Programming with Mathematica*.
10. Grasman, J., 1987, *Asymptotic Methods for Relaxation Oscillations and Applications*.
11. Grasman, J., Veling, E.J.M. and Willems, G.M., 1976, Relaxations Oscillations Governed by a van der Pol Equation, *SIAM Journal on Applied Mathematics*, 31, 667-676.
12. Graves-Morris, P. R. (Ed.), 1973, *Padé Approximants: Lectures delivered at a summer school held at the University of Kent, July 1972*.
13. Graves-Morris, P. R., and Baker, G. A. , 1996, *Padé Approximants*, 2nd Ed.
14. Jordan, D. W., and Smith, P., 1987, *Nonlinear Ordinary Differential Equations*, 2nd Ed.
15. LaSalle, J.P., 1949, Relaxation Oscillations, *Quarterly of Applied Mathematics*, 7.
16. Magnus, W., and Winkler, S., 1966, *Hill's Equation*.
17. Nayfeh, A., 1983, *Perturbation Methods*.
18. Rand, R.H. and Holmes, P.J., 1980, Bifurcation of Periodic Motions in Two Weakly Coupled van der Pol Oscillators, *International Journal of Non-Linear Mechanics*, 15, 387-399.
19. Reinhall, P.G. and Storti, D.W., 1995, A Numerical Investigation of Phase-Locked and Chaotic Behavior of Coupled van der Pol Oscillators, *Proceedings of the 15th Biennial ASME Conference on Mechanical Vibration and Noise*.

20. Reinhall, P.G., Storti, D.W. and Sliger, D.M., 1997, in submission, Asymmetric Dynamics of Coupled van der Pol Oscillators, *ASME Journal of Vibrations and Acoustics*.
21. Stoker, J.J., 1950, *Nonlinear Vibrations in Mechanical and Electrical Systems*.
22. Storti, D. 1984, *Coupled Relaxation Oscillators: Stability of Phase-Locked Modes* (Ph.D. Thesis, Cornell University.)
23. Storti, D. W., Nevrinceanu, C., and Reinhall, P.G., 1993, *Perturbation Solution of an Oscillator with Periodic van der Pol Damping*.
24. Storti, D.W., and Rand, R.H., 1982, Dynamics of Two Strongly Coupled van der Pol Oscillators, *International Journal of Non-Linear Mechanics*, 17, 143-152.
25. Storti, D.W., and Rand, R.H., 1986, Dynamics of Two Strongly Coupled van der Pol Oscillators, *SIAM Journal on Applied Mathematics*, 46, 56-67.
26. Storti, D.W., and Reinhall, P. G., 1993, *Stability of In-Phase and Out-of-Phase Modes for a Pair of Linearly Coupled van der Pol Oscillators*.
27. Storti, D.W., and Reinhall, P. G., 1996, *Hill's Equation Analysis of Phase-Locked Mode Stability for Coupled van der Pol Oscillators*.
28. van der Pol, B. and van der Mark, J., 1928, The Heartbeat Considered as a Relaxation Oscillation, and an Electrical Model of the Heart, *Philosophical Magazine*, 7, 763-775.
29. van der Pol, B., 1926, On Relaxation Oscillations, *Philosophical Magazine*, 7, 978-992.
30. van der Pol, B., 1927, Forced Oscillations in a Circuit with Nonlinear Resistance (Receptance with Reactive Triode), *Selected Papers on Mathematical Trends in Control Theory*, Bellman and Kalaba, Editors.
31. Van Dyke, M., 1975, *Perturbation Methods in Fluid Mechanics*.
32. Wolfram, S., 1994, *Mathematica: The Student Book*.

APPENDIX A: MATHEMATICA™ CODE FOR VDP EQUATION

This first block of code produces the first three terms of the of the VDP equation. Comments are included to help clarify the procedure. A second set of code is included which will start with a certain number of terms already in the solution and calculate two more terms. That code can be used to extend the solution as far as the user wants or until the computer runs out of memory.

STARTER PROGRAM

```
$Line = ∞;
SetDirectory["c:\\vdp\\complex\\odata"]

(* pmult[f,g,x,n] multiplies power series f by power series g
   where x is the variable, and keeps only through order n *)
pmult[f_, g_, x_Symbol, n_Integer] := Sum[Sum[x^{i+j} Coefficient[f, x, i] Coefficient[g, x, j],
   {i, 0, n}], {j, 0, n-1}]

(* getX[n] creates a power series in e of order n with argument x[i,t] *)
getX[n_] := Expand[Sum[e^i x[i, t], {i, 0, n}]

(* xeven[] and xodd[] assign x[i,t] to be a complex cosine or sign *)
xeven[i_] := Sum[A[i, j] (z^j + z^{-j}),
   {j, 1, 2 i + 1}, △ j = 2]
xodd[i_] := Sum[I A[i, j] (z^j - z^{-j}),
   {j, 1, 2 i + 1}, △ j = 2]

(* getW[n] creates the frequency power series *)
getW[n_] := 1 + Sum[e^i w[i],
   {i, 2, n}, △ i = 2]
```



```

(* noslope[] enforces the boundary condition in Equation (1-1) *)
noslope[i_] := Module[{temp}, temp = Coefficient[X[t], e, i];
  Solve[(myD[temp] /. Z → 1) == 0, A[i, 1]]]

(* myD[] and myD2[] are specialized derivatives *)
myD[f_] := f /. {Za → I a Za, Z → I Z}
myD2[f_] := myD[myD[f]]

ClearAll[x, w, X, W, temp, lhs, rhs, A, B, i]; (* start with clean slate *)
n = 3; (* order of solution *)
X[t] = getX[n]; (* build power series in e *)
W = getW[n];

(* build the right hand sides of Eq 1-5 *)
rhs = pmult[e, pmult[W, pmult[∂tX[t], 1 - pmult[X[t], X[t], e, n - 1], e, n - 1],
  e, n - 1], e, n];
lhs = pmult[pmult[W, W, e, n] - 1, ∂{t,2}X[t], e, n];

(* assign x[i,t] form to match Eq 1-15 *)
Table[x[i, t] = xeven[i], {i, 0, n, 2}];
Table[x[i, t] = xodd[i], {i, 1, n, 2}];

(* back to building right hand sides *)
mid = rhs - lhs /. Table[x(0,1)[i, t] → myD[x[i, t]], {i, 0, n}];
mid = mid /. Table[x(0,2)[i, t] → myD2[x[i, t]], {i, 0, n}];
X[t] = X[t];

(* pull out each right hand side for each order of e *)
temp = Table[Coefficient[mid, e, i], {i, 1, n}];

(* free up some memory *)
ClearAll[lhs, rhs, mid, x];

```



```

(* Solving the 1st order equation *)
i = 1;
right = Collect[Expand[ $\frac{\text{temp}[i]}{I}$ ], Table[z2j+1, {j, 0, i}]];
sec = Expand[Coefficient[right, Z]]; (* Identifies the secular terms *)
solRule = Solve[sec == 0, A[0, 1]]; (* Suppresses secularity *)
A[0, 1] = A[0, 1] /. solRule[3];
right = right /. solRule[3];
Table[A[i, 2j+1] =  $\frac{\text{Coefficient}[\text{right}, z^{2j+1}]}{1 - (2j+1)^2}$ , {j, 1, i}]; (* Enforces Eq 1-15 *)
A[i, 1] = A[i, 1] /. noslope[i][1]; (* Enforces boundary condition *)
temp[i] = 0;

(* Solving the 2nd order equation *)
i = 2;
right = Collect[Expand[temp[i]], Table[z2j+1, {j, 0, i}]];
solRule = Solve[Expand[Coefficient[right, Z]] == 0, w[i]]; (* Id's the secular terms *)
w[i] = w[i] /. solRule[1];
right = right /. solRule[1];
Table[A[i, 2j+1] =  $\frac{\text{Coefficient}[\text{right}, z^{2j+1}]}{1 - (2j+1)^2}$ , {j, 1, i}]; (* Enforces Eq 1-15 *)
temp[i] = 0;

(* Solving the 3rd order equation *)
i = 3;
right = Collect[Expand[ $\frac{\text{temp}[i]}{I}$ ], Table[z2j+1, {j, 0, i}]];
solRule = Solve[Expand[Coefficient[right, Z]] == 0, A[i-1, 1]]; (* Id's the secular terms *)
A[i-1, 1] = A[i-1, 1] /. solRule[1];
right = right /. solRule[1];
Table[A[i, 2j+1] =  $\frac{\text{Coefficient}[\text{right}, z^{2j+1}]}{1 - (2j+1)^2}$ , {j, 1, i}]; (* Enforces Eq 1-15 *)
A[i, 1] = A[i, 1] /. noslope[i][1]; (* Enforces boundary condition *)
temp[i] = 0;

```



```

(* Saving the data... *)
DeleteFile["afile.txt"]
Save["afile.txt", A]
DeleteFile["wfile.txt"]
Save["wfile.txt", w]
DeleteFile["nfile.txt"]
Save["nfile.txt", n]

(* This section puts the coefficients back in a
form to use with sines and cosines...*)
Table[Table[B[i, j] = 2A[i, j], {j, 1, 2i+1, 2}], {i, 0, n, 2}];
Table[Table[B[i, j] = -2A[i, j], {j, 1, 2i+1, 2}], {i, 1, n, 2}];
Save["bfile.txt", B]

(* Rebuilding X[t] in terms of sines and cosines *)
Table[x[i, t] = Sum[B[i, j] Cos[j t], {j, 1, 2i+1}], {i, 0, n, 2}];

$$\Delta_{j=2}$$

Table[x[i, t] = Sum[B[i, j] Sin[j t], {j, 1, 2i+1}], {i, 1, n, 2}];

$$\Delta_{j=2}$$

X[t] = Sum[x[i, t] e^i, {i, 0, n}];

(* Check out the work... *)
W
X[t]

```

CONTINUATION PROGRAM

The continuation program uses the same functions defined above, and the code is identical down through defining **noslope[]** then change the code as follows:


```

ClearAll[x, w, X, W, temp, lhs, rhs, A, i, n];
n << "nfile.txt";
old = n;
n = old + 2;
Print["Starting, old = ", old, " new = ", n]
t1 = TimeUsed[];
X[t] = getX[n];
W = getW[n];
rhs = 1 - pmult[X[t], X[t], e, n - 1];
temp = pmult[W, \partial_t X[t], e, n - 1];
rhs = pmult[rhs, temp, e, n - 1];
Clear[temp];
rhs = rhs /. Table[e^i → a^i, {i, old, n - 1}];
rhs = rhs /. e → 0;
rhs = rhs /. a → e;
rhs = pmult[e, rhs, e, n];
lhs = pmult[W, W, e, n];
lhs = lhs - 1;
lhs = pmult[lhs, \partial_{(t,2)} X[t], e, n];
lhs = lhs /. Table[e^i → a^i, {i, old + 1, n}];
lhs = lhs /. e → 0;
lhs = lhs /. a → e;
Table[x[i, t] = xeven[i], {i, 0, n, 2}];
Table[x[i, t] = xodd[i], {i, 1, n, 2}];
mid = rhs - lhs /. Table[x^(0,1)[i, t] → myD[x[i, t]], {i, 0, n}];
mid = mid /. Table[x^(0,2)[i, t] → myD2[x[i, t]], {i, 0, n}];
Print["updating X[t] ..."]
X[t] = X[t];
Print["building temp..."]
temp = {mid /. {e^{old+1} → 1, e → 0}, mid /. {e^{old+2} → 1, e → 0}};
ClearAll[lhs, rhs, mid, x];
A << "afile.txt";
w << "wfile.txt";

```



```

i = old+1;
rhs = Collect[Expand[temp[1]], Table[Z^{2j+1}, {j, 0, i}]];
solRule = Solve[Expand[Coefficient[rhs, Z]] == 0, w[i]];
w[i] = w[i] /. solRule[[1]];
rhs = rhs /. solRule[[1]];
Table[A[i, 2j+1] =  $\frac{\text{Coefficient}[rhs, Z^{2j+1}]}{1 - (2j+1)^2}$ , {j, 1, i}];
temp[1] = 0;
i = old+2;
rhs = Collect[Expand[ $\frac{\text{temp}[2]}{I}$ ], Table[Z^{2j+1}, {j, 0, i}]];
solRule = Solve[Expand[Coefficient[rhs, Z]] == 0, A[i-1, 1]];
A[i-1, 1] = A[i-1, 1] /. solRule[[1]];
rhs = rhs /. solRule[[1]];
Table[A[i, 2j+1] =  $\frac{\text{Coefficient}[rhs, Z^{2j+1}]}{1 - (2j+1)^2}$ , {j, 1, i}];
A[i, 1] = A[i, 1] /. noslope[i][1];
temp[2] = 0;
DeleteFile[{"afile.txt", "wfile.txt", "nfile.txt"}]
Save["afile.txt", A]
Save["wfile.txt", w]
Save["nfile.txt", n]

```

From here the last few routines in the starter program can again be used to translate the solution back into sines and cosines and save the results in that form.

APPENDIX B: STABILITY TRANSITION CODE

The first program is “Recover.nb” which converts the coefficients of the complex VDP solution into real coefficients for use in the stability routines. It also calculates the ZMD surface coefficients. It updates these coefficients in the c:\stabil\data folder as well as the frequency coefficients. This code needs to be run only once after generating as many terms in the VDP solution as necessary.

RECOVER.NB

Directory structure is assumed to be

c:

-complex
- stabil

THIS HAS THE VDP SOLUTION STORED IN IT
DATA FOR THE STABILITY CURVES

```
$Line = ∞;
SetDirectory[ "c:\\\\vdp" ];
n << "complex\\\\odata\\\\nfile.txt"; (* number of terms available in VDP solution *)
Reads in solution to complex solution and converts them to coefficients for real solution
A << "complex\\\\odata\\\\afile.txt";
Table[Table[B[i, j] = 2 A[i, j], {j, 1, 2 i + 1, 2}], {i, 0, n, 2}];
Table[Table[B[i, j] = -2 A[i, j], {j, 1, 2 i + 1, 2}], {i, 1, n, 2}];
DeleteFile[ "complex\\\\odata\\\\bfile.txt" ];
DeleteFile[ "stabil\\\\data\\\\bfile.txt" ];
Save[ "complex\\\\odata\\\\bfile.txt", B];
Save[ "stabil\\\\data\\\\bfile.txt", B];
```

The next four lines calculate the coefficients of the ZMD surface

```
Table[x[i] = Sum[1/2 B[i, j] (Z^j + Z^-j), {j, 0, n, 2}];
      △ j=2
Table[x[i] = Sum[-1/2 I B[i, j] (Z^j - Z^-j), {j, 1, n, 2}];
      △ j=2
Table[b[i] = Sum[(Expand[-1/2 x[j] x[i-j]] /. Z → 0)], {j, 0, i}], {i, 0, n, 2}];
b[0] = b[0] + 1/2;
```

Saves the ZMD coefficients, updates the frequency coefficients in the stabil folder and updates how many terms are available in the VDP for the stability routines


```

DeleteFile["stabil\\data\\crit.txt"]
Save["stabil\\data\\crit.txt", b]
DeleteFile["stabil\\data\\wfile.txt"]
CopyFile["complex\\odata\\wfile.txt", "stabil\\data\\wfile.txt"]
DeleteFile["stabil\\data\\nfile.txt"]
Save["stabil\\data\\nfile.txt", n]

```

The next program will start the solution for the stability transition curve:

STARTER.NB

Assumes the same directory structure as Recover.nb

```

$Line = ∞
SetDirectory[ "c:\\vdp\\stabil\\data"]

```

`pmult[]` is the same as in the VDP code. `getV[]` is equivalent to `getX[]` from VDP and `getA[]` makes the power series for the transition curve.

```

pmult[f_, g_, x_Symbol, n_Integer] :=  $\sum_{i=0}^n \sum_{j=0}^{n-i} x^{i+j} \text{Coefficient}[f, x, i] \text{Coefficient}[g, x, j]$ 
getV[order_] :=  $\sum_{n=0}^{\text{order}} e^n v[n, t]$ 
getA[order_] :=  $\sum_{n=0}^{\text{order}} e^n a[n]$ 

```

`update[]` updates the RHSs of Equation (5-12) as each `v[i,t]` is determined.

```

update[temp_, i_] := Module[{ttt}, ttt = temp;
  ttt[[i - 1]] = 0;
  Table[ttt[[i]] = ttt[[i]] /. v[j, t] → v[j, t], {j, 0, i - 1}];
  Table[ttt[[i]] = ttt[[i]] /. v(0,1)[j, t] → ∂tv[j, t], {j, 0, i - 1}];
  Table[ttt[[i]] = ttt[[i]] /. v(0,2)[j, t] → ∂(t,2)v[j, t], {j, 0, i - 1}];
  ttt]

```

Specialized ODE solver discussed in Chapter 5.


```

mysolve[i_, right_] := Module[{n, temp},
  n = 2 (i + 1) + 1;
  temp = c[i] Cos[k t] + s[i] Sin[k t];
  temp = temp + Sum[Coefficient[right, Cos[m t]] Cos[m t], {m, 1, k - 1}]/(-m^2 + k^2);
  temp = temp + Sum[Coefficient[right, Cos[m t]] Cos[m t], {m, k + 1, n}]/(-m^2 + k^2);
  temp = temp + Sum[Coefficient[right, Sin[m t]] Sin[m t], {m, 1, k - 1}]/(-m^2 + k^2);
  temp = temp + Sum[Coefficient[right, Sin[m t]] Sin[m t], {m, k + 1, n}]/(-m^2 + k^2);
  temp]

```

Build the power series for the frequency, W, the VDP solution, U, and the ZMD surface, B.

```

W = 1 + Sum[e^i w[i], {i, 2, 5}] /. i -> 2;
U = Sum[e^i u[i, t], {i, 0, 5}];
B = Sum[e^i b[i], {i, 0, 5}] /. i -> 2;
ClearAll[n, v, V, A, a, temp, right, s, c]
n = 5; (* how many terms to calculate *)
V[t] = getV[n];
A = getA[n];
a[0] = 0; (* which value of a[0] to go after *)
k = Sqrt[1 + 2 a[0]]; (* k of Eq (5-6) *)

```

rhs is the right hand side of Equation (5-12) prior to separating the powers of e. Once they are separated, each power is stored in temp[i].

```

rhs = pmult[pmult[e W, D[t] V[t], e, n], 1 - pmult[U, U, e, n - 1] - 2 B, e, n] -
  2 pmult[A - a0, V[t], e, n] - pmult[pmult[W, W, e, n] - 1, D[t, 2] V[t], e, n];
temp = Table[Coefficient[rhs, e, i], {i, 1, n}];
Clear[rhs];

```

Read in the coefficients for VDP, frequency and ZMD surface (generated by recover.nb).


```
u << "newu.txt";
w << "wfile.txt";
b << "crit.txt";
```

Solve the zeroeth order equation, note the rhs is zero for this equation. Last line is the condition of unit displacement for the perturbation. It can be replaced with other conditions or left out entirely.

```
i = 0;
v[i, t] = mysolve[i, 0];
v[i, t] = v[i, t] /. Solve[(getV[i] /. t -> 0) == 1, c[i]][1];
```

Solve the first order equation. First update the rhs to reflect $v[0,t]$, next find the secular term coefficients, $s1$ and $c1$. Next solve to eliminate the secular terms, in this case for $a[1]$ and $s[0]$. Next update the coefficients and the rhs with the solution just found and finally call the specialized ODE solver to get $v[1,t]$. Again the last line imposes unit displacement and could be left out or replaced by other conditions.

Note: For this case, $a[0]=0$, picking $\text{sol}[[1]]$ gives the lower curve while $\text{sol}[[2]]$ would give the upper curve.

```
i = 1;
temp = update[temp, i];
right = Collect[TrigReduce[temp[i]], {Sin[t], Cos[t]}];
s1 = Coefficient[right, Sin[t]];
c1 = Coefficient[right, Cos[t]];
sol = Solve[{s1 == 0, c1 == 0}, {a[i], s[i - 1]}]
a[i] = a[i] /. sol[[1]];
v[i - 1, t] = v[i - 1, t] /. sol[[1]];
s[i - 1] = s[i - 1] /. sol[[1]];
right = right /. sol[[1]];
v[i, t] = mysolve[i, right];
v[i, t] = v[i, t] /. Solve[(getV[i] /. t -> 0) == 1, c[i]][1];
```

Solve second order equation, just like above.

```
i = 2;
temp = update[temp, i];
right = Collect[TrigReduce[temp[i]], {Sin[t], Cos[t]}];
s1 = Coefficient[right, Sin[t]];
c1 = Coefficient[right, Cos[t]];
sol = Solve[{s1 == 0, c1 == 0}, {a[i], s[i - 1]}]
a[i] = a[i] /. sol[[1]];
s[i - 1] = s[i - 1] /. sol[[1]];
right = right /. sol[[1]];
```



```
v[i, t] = mysolve[i, right];
v[i, t] = v[i, t] /. Solve[(getV[i] /. t -> 0) == 1, c[i]][1];
```

Same thing for third order...

```
i = 3;
temp = update[temp, i];
right = Collect[TrigReduce[temp[[i]]], {Sin[t], Cos[t]}];
s1 = Coefficient[right, Sin[t]];
c1 = Coefficient[right, Cos[t]];
sol = Solve[{s1 == 0, c1 == 0}, {a[i], s[i - 1]}]
a[i] = a[i] /. sol[[1]];
s[i - 1] = s[i - 1] /. sol[[1]];
right = right /. sol[[1]];
v[i, t] = mysolve[i, right];
v[i, t] = v[i, t] /. Solve[(getV[i] /. t -> 0) == 1, c[i]][1];
```

Same thing for fourth order...

```
i = 4;
temp = update[temp, i];
right = Collect[TrigReduce[temp[[i]]], {Sin[t], Cos[t]}];
s1 = Coefficient[right, Sin[t]];
c1 = Coefficient[right, Cos[t]];
sol = Solve[{s1 == 0, c1 == 0}, {a[i], s[i - 1]}]
a[i] = a[i] /. sol[[1]];
s[i - 1] = s[i - 1] /. sol[[1]];
right = right /. sol[[1]];
v[i, t] = mysolve[i, right];
v[i, t] = v[i, t] /. Solve[(getV[i] /. t -> 0) == 1, c[i]][1];
```

Same thing for fifth order...

```
i = 5;
temp = update[temp, i];
right = Collect[TrigReduce[temp[[i]]], {Sin[t], Cos[t]}];
s1 = Coefficient[right, Sin[t]];
c1 = Coefficient[right, Cos[t]];
sol = Solve[{s1 == 0, c1 == 0}, {a[i], s[i - 1]}]
a[i] = a[i] /. sol[[1]];
s[i - 1] = s[i - 1] /. sol[[1]];
right = right /. sol[[1]];
v[i, t] = mysolve[i, right];
v[i, t] = v[i, t] /. Solve[(getV[i] /. t -> 0) == 1, c[i]][1];
```


Save the results. a01.txt is the lower curve out of a[0]=0. n01.txt is how many terms of v[i,t] have been solved.

```
DeleteFile["a01.txt"]
Save["a01.txt", A]
DeleteFile["v01.txt"]
Save["v01.txt", V]
DeleteFile["n01.txt"]
Save["n01.txt", n]
```

CONTINUE.NB

Continue will take the results of either starter.nb, or itself and extend the results by four terms. The functions down through and including mysolve[] from starter.nb need to be included as well as MyExpand[] which uses Euler's identity to update the right hand side of Equation (5-12) more quickly:

```
MyExpand[mess_] := Module[{Z, temp},
  temp = Expand[mess /. {Cos[m_t] ->  $\frac{1}{2} (Z^m + Z^{-m})$ , Sin[m_t] ->  $-\frac{1}{2} I (Z^m - Z^{-m})$ ,
    Cos[t] ->  $\frac{1}{2} (Z + \frac{1}{Z})$ , Sin[t] ->  $-\frac{1}{2} I (Z - \frac{1}{Z})$ }];
  Expand[temp /. {Zm -> Cos[m t] + I Sin[m t], Z2 -> Cos[2 t] + I Sin[2 t],
    Z -> Cos[t] + I Sin[t]}]]
```

The next section of code checks to ensure enough terms are available in the VDP solution and then builds the right hand sides of Equation (5-12) much as above. It prints out lines to let the user know what order terms it is trying to calculate:

```
n << "nfile.txt";
m = n;
Print[m, " terms in VDP solution available."]
n << "n01.txt";
min = n + 1;
n = min + 3;
Print["Starting with ", min, ", going to ", n, "."]
If[n > m, Print["Not enough terms!!"]; Quit[], Clear[m]]
```



```

W = 1 +  $\sum_{\substack{i=2 \\ \Delta i=2}}^n e^i w[i];$ 
U =  $\sum_{i=0}^n e^i u[i, t];$ 
ZMD =  $\sum_{\substack{i=0 \\ \Delta i=2}}^n e^i b[i];$ 
ClearAll[v, V, A, temp, rhs, s, c]
V[t] = getV[n];
A = getA[n];
rhs = pmult[e W, \partial_t V[t], e, n];
temp = 1 - pmult[U, U, e, n] - 2 ZMD;
rhs = pmult[rhs, temp, e, n, min];
temp = 2 pmult[A - a[0], V[t], e, n, min];
temp2 = pmult[W, W, e, n] - 1;
temp2 = pmult[temp2, \partial_{(t,2)} V[t], e, n, min];
rhs = rhs - temp - temp2;
ClearAll[temp, temp2];
temp = Table[Coefficient[rhs, e, i], {i, min, n}];
Clear[rhs];
<< "a01.txt";
<< "v01.txt";
k =  $\sqrt{1 + 2 a[0]};$ 
Table[u[i, t] =  $\sum_{\substack{j=1 \\ \Delta j=2}}^{2i+1} B[i, j] \cos[j t], \{i, 0, n, 2\}\right];$ 
Table[u[i, t] =  $\sum_{\substack{j=1 \\ \Delta j=2}}^{2i+1} B[i, j] \sin[j t], \{i, 1, n, 2\}\right];$ 
B << "bfile.txt";
w << "wfile.txt";
b << "crit.txt";

```

The next section calculates the four new terms, and are just like the equivalent sections of starter.nb except for using MyExpand[] instead of Expand[]:

```

i = min;
Print["Working on term: ", i]
temp = update[temp, i];
rhs = MyExpand[temp[[i - min + 1]]];

```



```

s1 = Coefficient[rhs, Sin[k t]] ;
c1 = Coefficient[rhs, Cos[k t]] ;
sol = Solve[{s1 == 0, c1 == 0}, {a[i], s[i - 1]}] ;
a[i] = a[i] /. sol[[1]] ;
s[i - 1] = s[i - 1] /. sol[[1]] ;
rhs = rhs /. sol[[1]] ;
v[i, t] = mysolve[i, rhs] ;
v[i, t] = v[i, t] /. Solve[(getV[i] /. t → 0) == 1, c[i]][[1]] ;

i = min + 1;
Print["Working on term: ", i]
temp = update[temp, i];
rhs = MyExpand[temp[[i - min + 1]]];
s1 = Coefficient[rhs, Sin[k t]] ;
c1 = Coefficient[rhs, Cos[k t]] ;
sol = Solve[{s1 == 0, c1 == 0}, {a[i], s[i - 1]}] ;
a[i] = a[i] /. sol[[1]] ;
s[i - 1] = s[i - 1] /. sol[[1]] ;
rhs = rhs /. sol[[1]] ;
v[i, t] = mysolve[i, rhs] ;
v[i, t] = v[i, t] /. Solve[(getV[i] /. t → 0) == 1, c[i]][[1]] ;

i = min + 2;
Print["Working on term: ", i]
temp = update[temp, i];
rhs = MyExpand[temp[[i - min + 1]]];
s1 = Coefficient[rhs, Sin[k t]] ;
c1 = Coefficient[rhs, Cos[k t]] ;
sol = Solve[{s1 == 0, c1 == 0}, {a[i], s[i - 1]}] ;
a[i] = a[i] /. sol[[1]] ;
s[i - 1] = s[i - 1] /. sol[[1]] ;
rhs = rhs /. sol[[1]] ;
v[i, t] = mysolve[i, rhs] ;
v[i, t] = v[i, t] /. Solve[(getV[i] /. t → 0) == 1, c[i]][[1]] ;

i = min + 3;
Print["Working on term: ", i]
temp = update[temp, i];
rhs = MyExpand[temp[[i - min + 1]]];
s1 = Coefficient[rhs, Sin[k t]] ;
c1 = Coefficient[rhs, Cos[k t]] ;
sol = Solve[{s1 == 0, c1 == 0}, {a[i], s[i - 1]}] ;

```



```
a[i] = a[i] /. sol[[1]];
s[i-1] = s[i-1] /. sol[[1]];
rhs = rhs /. sol[[1]];
v[i, t] = mysolve[i, rhs];
v[i, t] = v[i, t] /. Solve[(getV[i] /. t → 0) == 1, c[i]][[1]];
```

Finally save the results as above:

```
A = getA[n];
V[t] = getV[n];
DeleteFile["a01.txt"]
Save["a01.txt", a]
DeleteFile["v01.txt"]
Save["v01.txt", v]
DeleteFile["n01.txt"]
Save["n01.txt", n]
```


APPENDIX C: SOLUTION TO VDP EQUATION

The analytical solution to Equation (1-1) through order ϵ^{10} :

$$\begin{aligned}
 x[t] = & 2 \cos[t] + \epsilon^2 \left(-\frac{\cos[t]}{8} + \frac{3}{16} \cos[3t] - \frac{5}{96} \cos[5t] \right) + \\
 & \epsilon^4 \left(\frac{73 \cos[t]}{12288} - \frac{47 \cos[3t]}{1536} + \frac{1085 \cos[5t]}{27648} - \frac{2149 \cos[7t]}{110592} + \frac{61 \cos[9t]}{20480} \right) + \\
 & \epsilon^6 \left(\frac{6479 \cos[t]}{6635520} + \frac{48437 \cos[3t]}{35389440} - \frac{259945 \cos[5t]}{31850496} + \right. \\
 & \quad \frac{4253767 \cos[7t]}{398131200} - \frac{480523 \cos[9t]}{73728000} + \frac{4937537 \cos[11t]}{2654208000} - \frac{715247 \cos[13t]}{3715891200} \Big) + \\
 & \epsilon^8 \left(-\frac{377080601 \cos[t]}{1712282664960} + \frac{36921629 \cos[3t]}{71345111040} + \frac{4094345 \cos[5t]}{9172942848} - \right. \\
 & \quad \frac{107409503789 \cos[7t]}{45864714240000} + \frac{188691979247 \cos[9t]}{59454259200000} - \frac{2067847855711 \cos[11t]}{936404582400000} + \\
 & \quad \frac{1114925731231 \cos[13t]}{1310966415360000} - \frac{784260289 \cos[15t]}{4661213921280} + \frac{392636471 \cos[17t]}{29964946636800} \Big) + \\
 & \epsilon^{10} \left(-\frac{44898976356847 \cos[t]}{3020466620989440000} - \frac{4475878408049 \cos[3t]}{50341110349824000} + \right. \\
 & \quad \frac{511229379671 \cos[5t]}{2958824445050880} + \frac{21294508407929 \cos[7t]}{165112971264000000} - \frac{1838562603094127 \cos[9t]}{2621932830720000000} + \\
 & \quad \frac{129978704206760957 \cos[11t]}{1321454146682880000000} - \frac{11188471201628174701 \cos[13t]}{14800286442848256000000} + \\
 & \quad \frac{27736422934204291 \cos[15t]}{78934861028524032000} - \frac{148525877527816577 \cos[17t]}{1522315176978677760000} + \\
 & \quad \frac{1600597132693073 \cos[19t]}{108736798355619840000} - \frac{29654422883 \cos[21t]}{32288758824960000} \Big) + \\
 & \epsilon \left(\frac{3 \sin[t]}{4} - \frac{1}{4} \sin[3t] \right) + \epsilon^3 \left(-\frac{7 \sin[t]}{256} + \frac{21}{256} \sin[3t] - \frac{35}{576} \sin[5t] + \frac{7}{576} \sin[7t] \right) + \\
 & \epsilon^5 \left(-\frac{12971 \sin[t]}{4423680} - \frac{2591 \sin[3t]}{294912} + \right. \\
 & \quad \frac{52885 \sin[5t]}{2654208} - \frac{110621 \sin[7t]}{6635520} + \frac{7457 \sin[9t]}{1228800} - \frac{5533 \sin[11t]}{7372800} \Big) + \\
 & \epsilon^7 \left(\frac{33114653 \sin[t]}{44590694400} - \frac{82937 \sin[3t]}{212336640} - \frac{1939625 \sin[5t]}{764411904} + \frac{1061235889 \sin[7t]}{191102976000} - \right. \\
 & \quad \frac{179467921 \sin[9t]}{35389440000} + \frac{223342933 \sin[11t]}{92897280000} - \frac{195050323 \sin[13t]}{346816512000} + \frac{138697 \sin[15t]}{2774532096} \Big) + \\
 & \epsilon^9 \left(\frac{9822191352131 \sin[t]}{251705551749120000} + \frac{89866136849 \sin[3t]}{342456532992000} - \frac{1702014109 \sin[5t]}{12328435187712} - \right. \\
 & \quad \frac{2088126932941 \sin[7t]}{2751882854400000} + \frac{41070940258801 \sin[9t]}{24970788864000000} - \frac{1694102483205143 \sin[11t]}{1048773132288000000} + \\
 & \quad \frac{662514241768639 \sin[13t]}{734141192601600000} - \frac{507370714969 \sin[15t]}{1740186530611200} + \frac{15080405867887 \sin[17t]}{302046662098944000} - \\
 & \quad \frac{466445839 \sin[19t]}{134842259865600} \Big)
 \end{aligned}$$

Frequency Expansion through order 20:

$$\omega = 1 - \frac{e^2}{16} + \frac{17e^4}{3072} + \frac{35e^6}{884736} - \frac{678899e^8}{5096079360} +$$

$$-\frac{28160413e^{10}}{2293235712000} + \frac{16729607288111e^{12}}{3698530556313600000} - \frac{5722795344767278507e^{14}}{5219366321069752320000000}$$

$$+\frac{1846779765852173498887007e^{16}}{14731139504587268947968000000000} + \frac{3202506386889338212533493973243e^{18}}{415771681377471078787448832000000000000} -$$

$$-\frac{4038372199485064617691118289043994731e^{20}}{38724641786152554301399954253414400000000000000}$$

NUMERICAL RESULTS

These lists of numbers represent the coefficients of the cosine or sines of the VDP solution. $c[2]$ for example shows that $x_2(t) = -0.125 \cos(t) + 0.188 \sin(t) - 0.0521 t \cos(t)$.

Cosine Coefficients through order 25:

```

c[0]
{2.}
c[2]
{-0.125, 0.188, -0.0521}
c[4]
{0.00594, -0.0306, 0.0392, -0.0194, 0.00298}
c[6]
{0.000976, 0.00137, -0.00816, 0.0107, -0.00652, 0.00186, -0.000192}
c[8]
{-0.00022, 0.000518, 0.000446, -0.00234, 0.00317, -0.00221, 0.00085, -0.000168,
 0.0000131}
c[10]
{-0.0000149, -0.0000889, 0.000173, 0.000129, -0.000701, 0.000984, -0.000756,
 0.000351, -0.0000976, 0.0000147, -9.18×10-7}
c[12]
{0.000011, -0.0000129, -0.000034, 0.000059, 0.0000364, -0.000214, 0.000313,
 -0.00026, 0.000139, -0.0000479, 0.0000104, -1.26×10-6, 6.56×10-8}
c[14]
{-3.84×10-7, 5.51×10-6, -4.1×10-6, -0.0000121, 0.0000203, 9.83×10-6, -0.0000661,
 0.000101, -0.00009, 0.0000533, -0.0000216, 5.91×10-6, -1.04×10-6, 1.06×10-7,
 -4.75×10-9}
c[16]

```


$\{-5.56 \times 10^{-7}, 1.1 \times 10^{-7}, 2.13 \times 10^{-6}, -1.4 \times 10^{-6}, -4.24 \times 10^{-6}, 7.02 \times 10^{-6},$
 $2.46 \times 10^{-6}, -0.0000206, 0.000033, -0.0000312, 0.0000201, -9.22 \times 10^{-6}, 3. \times 10^{-6},$
 $-6.79 \times 10^{-7}, 1.01 \times 10^{-7}, -8.88 \times 10^{-9}, 3.47 \times 10^{-10}\}$

c[18]

$\{8.17 \times 10^{-8}, -3.22 \times 10^{-7}, -8.11 \times 10^{-9}, 7.85 \times 10^{-7}, -4.79 \times 10^{-7}, -1.46 \times 10^{-6},$
 $2.43 \times 10^{-6}, 5.36 \times 10^{-7}, -6.42 \times 10^{-6}, 0.0000108, -0.0000108, 7.52 \times 10^{-6},$
 $-3.81 \times 10^{-6}, 1.42 \times 10^{-6}, -3.85 \times 10^{-7}, 7.42 \times 10^{-8}, -9.55 \times 10^{-9}, 7.35 \times 10^{-10}, -2.55 \times 10^{-11}\}$

c[20]

$\{2.46 \times 10^{-8}, 2.84 \times 10^{-8}, -1.22 \times 10^{-7}, -1.12 \times 10^{-8}, 2.85 \times 10^{-7}, -1.65 \times 10^{-7}, -4.96 \times 10^{-7},$
 $8.45 \times 10^{-7}, 8.07 \times 10^{-8}, -2.01 \times 10^{-6}, 3.57 \times 10^{-6}, -3.76 \times 10^{-6}, 2.78 \times 10^{-6}, -1.53 \times 10^{-6},$
 $6.37 \times 10^{-7}, -2. \times 10^{-7}, 4.65 \times 10^{-8}, -7.78 \times 10^{-9}, 8.82 \times 10^{-10}, -6.05 \times 10^{-11}, 1.89 \times 10^{-12}\}$

c[22]

$\{-7.83 \times 10^{-9}, 1.68 \times 10^{-8}, 1.41 \times 10^{-8}, -4.49 \times 10^{-8}, -6.79 \times 10^{-9}, 1.02 \times 10^{-7}, -5.82 \times 10^{-8},$
 $-1.67 \times 10^{-7}, 2.94 \times 10^{-7}, -7.04 \times 10^{-9}, -6.26 \times 10^{-7}, 1.18 \times 10^{-6}, -1.3 \times 10^{-6},$
 $1.02 \times 10^{-6}, -6.05 \times 10^{-7}, 2.76 \times 10^{-7}, -9.72 \times 10^{-8}, 2.63 \times 10^{-8}, -5.35 \times 10^{-9},$
 $7.91 \times 10^{-10}, -8.01 \times 10^{-11}, 4.95 \times 10^{-12}, -1.41 \times 10^{-13}\}$

c[24]

$\{-7.03 \times 10^{-10}, -3.68 \times 10^{-9}, 6.03 \times 10^{-9}, 5.84 \times 10^{-9}, -1.63 \times 10^{-8}, -3.2 \times 10^{-9},$
 $3.61 \times 10^{-8}, -2.08 \times 10^{-8}, -5.57 \times 10^{-8}, 1.02 \times 10^{-7}, -1.41 \times 10^{-8}, -1.94 \times 10^{-7},$
 $3.89 \times 10^{-7}, -4.51 \times 10^{-7}, 3.74 \times 10^{-7}, -2.36 \times 10^{-7}, 1.16 \times 10^{-7}, -4.52 \times 10^{-8},$
 $1.38 \times 10^{-8}, -3.28 \times 10^{-9}, 5.92 \times 10^{-10}, -7.84 \times 10^{-11}, 7.17 \times 10^{-12}, -4.03 \times 10^{-13}, 1.05 \times 10^{-14}\}$

Sine Coefficients through order 25:

s[1]

$\{0.75, -0.25\}$

s[3]

$\{-0.0273, 0.082, -0.0608, 0.0122\}$

s[5]

$\{-0.00293, -0.00879, 0.0199, -0.0167, 0.00607, -0.00075\}$

s[7]

$\{0.000743, -0.000391, -0.00254, 0.00555, -0.00507, 0.0024, -0.000562, 0.00005\}$

s[9]

$\{0.000039, 0.000262, -0.000138, -0.000759, 0.00164, -0.00162, 0.000902,$
 $-0.000292, 0.0000499, -3.46 \times 10^{-6}\}$

s[11]

$\{-0.000035, -9.57 \times 10^{-6}, 0.0000953, -0.0000478, -0.000227, 0.000505, -0.000527,$
 $0.000332, -0.000132, 0.000032, -4.32 \times 10^{-6}, 2.45 \times 10^{-7}\}$

s[13]

$\{1.51 \times 10^{-6}, -0.0000106, -4.09 \times 10^{-6}, 0.0000335, -0.0000174, -0.0000683, 0.000158,$
 $-0.000175, 0.000121, -0.0000556, 0.000017, -3.3 \times 10^{-6}, 3.67 \times 10^{-7}, -1.76 \times 10^{-8}\}$

s[15]

$\{1.72 \times 10^{-6}, 1.56 \times 10^{-6}, -4.06 \times 10^{-6}, -1.73 \times 10^{-6}, 0.0000115, -6.5 \times 10^{-6},$
 $-0.0000206, 0.0000501, -0.0000583, 0.0000437, -0.0000225, 8.14 \times 10^{-6},$
 $-2.02 \times 10^{-6}, 3.26 \times 10^{-7}, -3.08 \times 10^{-8}, 1.28 \times 10^{-9}\}$

s[17]

$\{-2.66 \times 10^{-7}, 4.13 \times 10^{-7}, 6.46 \times 10^{-7}, -1.46 \times 10^{-6}, -6.44 \times 10^{-7}, 3.94 \times 10^{-6},$
 $-2.44 \times 10^{-6}, -6.16 \times 10^{-6}, 0.000016, -0.0000196, 0.0000157, -8.91 \times 10^{-6},$
 $3.66 \times 10^{-6}, -1.09 \times 10^{-6}, 2.26 \times 10^{-7}, -3.12 \times 10^{-8}, 2.56 \times 10^{-9}, -9.4 \times 10^{-11}\}$

s[19]

$\{-7.43 \times 10^{-8}, -1.34 \times 10^{-7}, 1.57 \times 10^{-7}, 2.59 \times 10^{-7}, -5.16 \times 10^{-7}, -2.24 \times 10^{-7}, 1.35 \times 10^{-6},$
 $-9.17 \times 10^{-7}, -1.83 \times 10^{-6}, 5.15 \times 10^{-6}, -6.62 \times 10^{-6}, 5.62 \times 10^{-6}, -3.45 \times 10^{-6},$
 $1.58 \times 10^{-6}, -5.37 \times 10^{-7}, 1.35 \times 10^{-7}, -2.41 \times 10^{-8}, 2.91 \times 10^{-9}, -2.11 \times 10^{-10}, 6.94 \times 10^{-12}\}$

s[21]

$\{2.47 \times 10^{-8}, -1.02 \times 10^{-8}, -5.54 \times 10^{-8}, 5.45 \times 10^{-8}, 9.78 \times 10^{-8}, -1.81 \times 10^{-7},$
 $-7.49 \times 10^{-8}, 4.59 \times 10^{-7}, -3.43 \times 10^{-7}, -5.37 \times 10^{-7}, 1.66 \times 10^{-6}, -2.24 \times 10^{-6},$
 $2.01 \times 10^{-6}, -1.32 \times 10^{-6}, 6.59 \times 10^{-7}, -2.51 \times 10^{-7}, 7.3 \times 10^{-8}, -1.59 \times 10^{-8},$
 $2.49 \times 10^{-9}, -2.66 \times 10^{-10}, 1.73 \times 10^{-11}, -5.15 \times 10^{-13}\}$

s[23]

$\{2.02 \times 10^{-9}, 9.52 \times 10^{-9}, -3.45 \times 10^{-9}, -2.18 \times 10^{-8}, 1.86 \times 10^{-8}, 3.59 \times 10^{-8},$
 $-6.37 \times 10^{-8}, -2.4 \times 10^{-8}, 1.56 \times 10^{-7}, -1.28 \times 10^{-7}, -1.54 \times 10^{-7}, 5.34 \times 10^{-7},$
 $-7.57 \times 10^{-7}, 7.15 \times 10^{-7}, -5. \times 10^{-7}, 2.69 \times 10^{-7}, -1.13 \times 10^{-7}, 3.69 \times 10^{-8},$
 $-9.34 \times 10^{-9}, 1.79 \times 10^{-9}, -2.5 \times 10^{-10}, 2.4 \times 10^{-11}, -1.41 \times 10^{-12}, 3.84 \times 10^{-14}\}$

s[25]

$\{-1.86 \times 10^{-9}, -4.12 \times 10^{-10}, 3.91 \times 10^{-9}, -8.87 \times 10^{-10}, -8.2 \times 10^{-9}, 6.36 \times 10^{-9}, 1.29 \times 10^{-8},$
 $-2.23 \times 10^{-8}, -7.37 \times 10^{-9}, 5.29 \times 10^{-8}, -4.73 \times 10^{-8}, -4.31 \times 10^{-8}, 1.72 \times 10^{-7},$
 $-2.56 \times 10^{-7}, 2.54 \times 10^{-7}, -1.87 \times 10^{-7}, 1.08 \times 10^{-7}, -4.9 \times 10^{-8}, 1.77 \times 10^{-8},$
 $-5.08 \times 10^{-9}, 1.14 \times 10^{-9}, -1.94 \times 10^{-10}, 2.45 \times 10^{-11}, -2.14 \times 10^{-12}, 1.15 \times 10^{-13}, -2.88 \times 10^{-15}\}$

APPENDIX D : SOLUTIONS TO THE VARIATIONAL EQUATION

This appendix includes the solutions to the variational equation through ϵ^5 for the cases covered in Chapter 5. Note that these solutions can be used to check if the code in Appendix C is working correctly.

Curves out of $A_0=0$:

$$\begin{aligned} \text{Lower} = & \cos[t] + \sin[t] + \epsilon \left(-\frac{\cos[t]}{8} + \frac{1}{8} \cos[3t] + \frac{3 \sin[t]}{8} - \frac{1}{8} \sin[3t] \right) + \\ & \epsilon^2 \left(-\frac{19 \cos[t]}{192} + \frac{1}{8} \cos[3t] - \frac{5}{192} \cos[5t] - \frac{7 \sin[t]}{192} + \frac{1}{16} \sin[3t] - \frac{5}{192} \sin[5t] \right) + \epsilon^3 \left(\frac{5 \cos[t]}{576} - \right. \\ & \left. \frac{7}{256} \cos[3t] + \frac{19}{768} \cos[5t] - \frac{7 \cos[7t]}{1152} - \frac{55 \sin[t]}{2304} + \frac{53}{768} \sin[3t] - \frac{89 \sin[5t]}{2304} + \frac{7 \sin[7t]}{1152} \right) + \\ & \epsilon^4 \left(\frac{4249 \cos[t]}{552960} - \frac{57 \cos[3t]}{2048} + \frac{3371 \cos[5t]}{110592} - \frac{2615 \cos[7t]}{221184} + \frac{61 \cos[9t]}{40960} + \frac{439 \sin[t]}{552960} - \right. \\ & \left. \frac{107 \sin[3t]}{9216} + \frac{1631 \sin[5t]}{110592} - \frac{1885 \sin[7t]}{221184} + \frac{61 \sin[9t]}{40960} \right) + \epsilon^5 \left(\frac{1013 \cos[t]}{7372800} + \right. \\ & \left. \frac{6707 \cos[3t]}{2211840} - \frac{40205 \cos[5t]}{5308416} + \frac{180211 \cos[7t]}{26542080} - \frac{40709 \cos[9t]}{14745600} + \frac{5533 \cos[11t]}{14745600} - \right. \\ & \left. \frac{8311 \sin[t]}{22118400} - \frac{21127 \sin[3t]}{2211840} + \frac{91811 \sin[5t]}{5308416} - \frac{319577 \sin[7t]}{26542080} + \frac{158179 \sin[9t]}{44236800} - \frac{5533 \sin[11t]}{14745600} \right) \end{aligned}$$

$$\begin{aligned} \text{Upper} = & \cos[t] - \sin[t] + \epsilon \left(\frac{\cos[t]}{8} - \frac{1}{8} \cos[3t] + \frac{3 \sin[t]}{8} - \frac{1}{8} \sin[3t] \right) + \\ & \epsilon^2 \left(-\frac{19 \cos[t]}{192} + \frac{1}{8} \cos[3t] - \frac{5}{192} \cos[5t] + \frac{7 \sin[t]}{192} - \frac{1}{16} \sin[3t] + \frac{5}{192} \sin[5t] \right) + \epsilon^3 \left(-\frac{5 \cos[t]}{576} + \right. \\ & \left. \frac{7}{256} \cos[3t] - \frac{19}{768} \cos[5t] + \frac{7 \cos[7t]}{1152} - \frac{55 \sin[t]}{2304} + \frac{53}{768} \sin[3t] - \frac{89 \sin[5t]}{2304} + \frac{7 \sin[7t]}{1152} \right) + \\ & \epsilon^4 \left(\frac{4249 \cos[t]}{552960} - \frac{57 \cos[3t]}{2048} + \frac{3371 \cos[5t]}{110592} - \frac{2615 \cos[7t]}{221184} + \right. \\ & \left. \frac{61 \cos[9t]}{40960} - \frac{439 \sin[t]}{552960} + \frac{107 \sin[3t]}{9216} - \frac{1631 \sin[5t]}{110592} + \frac{1885 \sin[7t]}{221184} - \frac{61 \sin[9t]}{40960} \right) + \\ & \epsilon^5 \left(-\frac{1013 \cos[t]}{7372800} - \frac{6707 \cos[3t]}{2211840} + \frac{40205 \cos[5t]}{5308416} - \frac{180211 \cos[7t]}{26542080} + \frac{40709 \cos[9t]}{14745600} - \frac{5533 \cos[11t]}{14745600} - \right. \\ & \left. \frac{8311 \sin[t]}{22118400} - \frac{21127 \sin[3t]}{2211840} + \frac{91811 \sin[5t]}{5308416} - \frac{319577 \sin[7t]}{26542080} + \frac{158179 \sin[9t]}{44236800} - \frac{5533 \sin[11t]}{14745600} \right) \end{aligned}$$

Curves out of $A_0=3/2$:

$$\begin{aligned}
\text{Lower} = & \cos[2t] + \epsilon^2 \left(-\frac{71}{576} \cos[2t] + \frac{23}{144} \cos[4t] - \frac{7}{192} \cos[6t] \right) + \\
& \epsilon^4 \left(\frac{15443 \cos[2t]}{1658880} - \frac{2809 \cos[4t]}{82944} + \frac{1427 \cos[6t]}{36864} - \frac{1127 \cos[8t]}{69120} + \frac{119 \cos[10t]}{55296} \right) + \\
& \epsilon^6 \left(\frac{11}{24} \sin[2t] - \frac{1}{6} \sin[4t] \right) + \epsilon^8 \left(-\frac{73 \sin[2t]}{1728} + \frac{47}{576} \sin[4t] - \frac{239 \sin[6t]}{4608} + \frac{5}{576} \sin[8t] \right) + \\
& \epsilon^{10} \left(-\frac{5407 \sin[2t]}{13271040} - \frac{112483 \sin[4t]}{9953280} + \frac{285299 \sin[6t]}{13271040} - \frac{65987 \sin[8t]}{4147200} + \frac{22187 \sin[10t]}{4423680} - \frac{1007 \sin[12t]}{1843200} \right)
\end{aligned}$$

$$\begin{aligned}
\text{Upper} = & \epsilon \left(-\frac{11}{48} \cos[2t] + \frac{1}{12} \cos[4t] \right) + \\
& \epsilon^3 \left(\frac{55 \cos[2t]}{1536} - \frac{181 \cos[4t]}{3456} + \frac{239 \cos[6t]}{9216} - \frac{5 \cos[8t]}{1152} \right) + \epsilon^5 \left(-\frac{319213 \cos[2t]}{79626240} + \right. \\
& \left. \frac{218417 \cos[4t]}{19906560} - \frac{378463 \cos[6t]}{26542080} + \frac{1117 \cos[8t]}{129600} - \frac{22187 \cos[10t]}{8847360} + \frac{1007 \cos[12t]}{3686400} \right) + \\
& \frac{1}{2} \sin[2t] + \epsilon^2 \left(-\frac{121 \sin[2t]}{1152} + \frac{23}{288} \sin[4t] - \frac{7}{384} \sin[6t] \right) + \\
& \epsilon^4 \left(\frac{46007 \sin[2t]}{3317760} - \frac{4385 \sin[4t]}{165888} + \frac{4883 \sin[6t]}{221184} - \frac{1127 \sin[8t]}{138240} + \frac{119 \sin[10t]}{110592} \right)
\end{aligned}$$

Curves out of A₀=4:

$$\begin{aligned}
\text{Lower} = & \cos[3t] - \sin[3t] + \\
& \epsilon \left(\frac{3 \cos[t]}{8} - \frac{3}{16} \cos[3t] - \frac{3}{16} \cos[5t] + \frac{3 \sin[t]}{8} + \frac{359}{240} \sin[3t] - \frac{3}{16} \sin[5t] \right) + \epsilon^2 \left(-\frac{329 \cos[t]}{640} + \right. \\
& \left. \frac{233 \cos[3t]}{1280} + \frac{479 \cos[5t]}{1280} - \frac{27}{640} \cos[7t] - \frac{51 \sin[t]}{128} - \frac{73913 \sin[3t]}{57600} - \frac{15}{256} \sin[5t] + \frac{27}{640} \sin[7t] \right) + \\
& \epsilon^3 \left(\frac{89813 \cos[t]}{153600} - \frac{76151 \cos[3t]}{230400} - \frac{139}{600} \cos[5t] - \frac{67 \cos[7t]}{2048} + \right. \\
& \left. \frac{469 \cos[9t]}{46080} + \frac{831 \sin[t]}{2048} + \frac{82393 \sin[3t]}{57600} + \frac{679 \sin[5t]}{5120} - \frac{5311 \sin[7t]}{51200} + \frac{469 \sin[9t]}{46080} \right) + \\
& \epsilon^4 \left(-\frac{385217 \cos[t]}{614400} + \frac{105987247 \cos[3t]}{309657600} + \right. \\
& \left. \frac{389277 \cos[5t]}{1638400} + \frac{30401 \cos[7t]}{409600} - \frac{327931 \cos[9t]}{11059200} + \frac{547 \cos[11t]}{215040} - \frac{273059 \sin[t]}{614400} - \right. \\
& \left. \frac{37616912581 \sin[3t]}{23224320000} - \frac{18809 \sin[5t]}{327680} + \frac{249571 \sin[7t]}{6144000} + \frac{27691 \sin[9t]}{2211840} - \frac{547 \sin[11t]}{215040} \right) + \\
& \epsilon^5 \left(\frac{42447078481 \cos[t]}{61931520000} - \frac{33657149027 \cos[3t]}{92897280000} - \frac{9222921259 \cos[5t]}{30965760000} - \frac{1330129 \cos[7t]}{39321600} + \right. \\
& \left. \frac{46069577 \cos[9t]}{9289728000} + \frac{88301 \cos[11t]}{20643840} - \frac{89371 \cos[13t]}{137625600} + \frac{400303339 \sin[t]}{825753600} + \frac{82024682603 \sin[3t]}{46448640000} + \right. \\
& \left. \frac{13130773 \sin[5t]}{206438400} - \frac{16057111 \sin[7t]}{589824000} - \frac{11346613 \sin[9t]}{371589120} + \frac{883481 \sin[11t]}{103219200} - \frac{89371 \sin[13t]}{137625600} \right)
\end{aligned}$$

$$\begin{aligned}
\text{Upper} = & \cos[3t] + \sin[3t] + \\
& \epsilon \left(-\frac{3 \cos[t]}{8} + \frac{3}{16} \cos[3t] + \frac{3}{16} \cos[5t] + \frac{3 \sin[t]}{8} + \frac{359}{240} \sin[3t] - \frac{3}{16} \sin[5t] \right) + \epsilon^2 \left(-\frac{329 \cos[t]}{640} + \right. \\
& \left. \frac{233 \cos[3t]}{1280} + \frac{479 \cos[5t]}{1280} - \frac{27}{640} \cos[7t] + \frac{51 \sin[t]}{128} + \frac{73913 \sin[3t]}{57600} + \frac{15}{256} \sin[5t] - \frac{27}{640} \sin[7t] \right) + \\
& \epsilon^3 \left(-\frac{89813 \cos[t]}{153600} + \frac{76151 \cos[3t]}{230400} + \frac{139}{600} \cos[5t] + \frac{67 \cos[7t]}{2048} - \right. \\
& \left. \frac{469 \cos[9t]}{46080} + \frac{831 \sin[t]}{2048} + \frac{82393 \sin[3t]}{57600} + \frac{679 \sin[5t]}{5120} - \frac{5311 \sin[7t]}{51200} + \frac{469 \sin[9t]}{46080} \right) + \\
& \epsilon^4 \left(-\frac{385217 \cos[t]}{614400} + \frac{105987247 \cos[3t]}{309657600} + \right. \\
& \left. \frac{389277 \cos[5t]}{1638400} + \frac{30401 \cos[7t]}{409600} - \frac{327931 \cos[9t]}{11059200} + \frac{547 \cos[11t]}{215040} + \frac{273059 \sin[t]}{614400} + \right. \\
& \left. \frac{37616912581 \sin[3t]}{23224320000} + \frac{18809 \sin[5t]}{327680} - \frac{249571 \sin[7t]}{6144000} - \frac{27691 \sin[9t]}{2211840} + \frac{547 \sin[11t]}{215040} \right) + \\
& \epsilon^5 \left(-\frac{42447078481 \cos[t]}{61931520000} + \frac{33657149027 \cos[3t]}{92897280000} + \frac{9222921259 \cos[5t]}{30965760000} + \frac{1330129 \cos[7t]}{39321600} - \right. \\
& \left. \frac{46069577 \cos[9t]}{9289728000} - \frac{88301 \cos[11t]}{20643840} + \frac{89371 \cos[13t]}{137625600} + \frac{400303339 \sin[t]}{825753600} + \frac{82024682603 \sin[3t]}{46448640000} + \right. \\
& \left. \frac{13130773 \sin[5t]}{206438400} - \frac{16057111 \sin[7t]}{589824000} - \frac{11346613 \sin[9t]}{371589120} + \frac{883481 \sin[11t]}{103219200} - \frac{89371 \sin[13t]}{137625600} \right)
\end{aligned}$$

APPENDIX E : STABILITY TRANSITION CURVES

This appendix includes the stability transition curves found in Chapter 5. Curves are given analytically through order 10 and numerically through order 30.

Curves out of $A_0=0$:

$$\begin{aligned} \text{Lower } \epsilon A = & -\frac{\epsilon}{2} + \frac{\epsilon^2}{8} + \frac{\epsilon^3}{32} - \frac{7\epsilon^4}{384} + \frac{3\epsilon^5}{1024} - \frac{247\epsilon^6}{442368} - \frac{11657\epsilon^7}{21233664} + \frac{1224811\epsilon^8}{2548039680} - \\ & \frac{65987129\epsilon^9}{611529523200} + \frac{248740367\epsilon^{10}}{36691771392000} \end{aligned}$$

Lower $\epsilon A =$

$$\begin{aligned} & -0.5\epsilon + 0.125\epsilon^2 + 0.03125\epsilon^3 - 0.018229\epsilon^4 + 0.0029297\epsilon^5 - \\ & 0.00055836\epsilon^6 - 0.00054899\epsilon^7 + 0.00048069\epsilon^8 - 0.00010791\epsilon^9 + 6.7792 \times 10^{-6}\epsilon^{10} + \\ & 0.000023325\epsilon^{11} - 0.000020161\epsilon^{12} + 3.8825 \times 10^{-6}\epsilon^{13} + 7.1301 \times 10^{-7}\epsilon^{14} - 1.1828 \times 10^{-6}\epsilon^{15} + \\ & 8.9935 \times 10^{-7}\epsilon^{16} - 1.1027 \times 10^{-7}\epsilon^{17} - 9.9766 \times 10^{-8}\epsilon^{18} + 6.0926 \times 10^{-8}\epsilon^{19} - 3.6467 \times 10^{-8}\epsilon^{20} + \\ & 1.5256 \times 10^{-11}\epsilon^{21} + 8.7439 \times 10^{-9}\epsilon^{22} - 2.8529 \times 10^{-9}\epsilon^{23} + 9.8924 \times 10^{-10}\epsilon^{24} + 3.551 \times 10^{-10}\epsilon^{25} - \\ & 6.2361 \times 10^{-10}\epsilon^{26} + 9.9193 \times 10^{-11}\epsilon^{27} + 2.5033 \times 10^{-11}\epsilon^{28} - 3.8338 \times 10^{-11}\epsilon^{29} + 3.6974 \times 10^{-11}\epsilon^{30} \end{aligned}$$

$$\begin{aligned} \text{Upper } \epsilon A = & \frac{\epsilon}{2} + \frac{\epsilon^2}{8} - \frac{\epsilon^3}{32} - \frac{7\epsilon^4}{384} - \frac{3\epsilon^5}{1024} - \frac{247\epsilon^6}{442368} + \frac{11657\epsilon^7}{21233664} + \frac{1224811\epsilon^8}{2548039680} + \\ & \frac{65987129\epsilon^9}{611529523200} + \frac{248740367\epsilon^{10}}{36691771392000} \end{aligned}$$

Upper $\epsilon A =$

$$\begin{aligned} & 0.5\epsilon + 0.125\epsilon^2 - 0.03125\epsilon^3 - 0.018229\epsilon^4 - 0.0029297\epsilon^5 - \\ & 0.00055836\epsilon^6 + 0.00054899\epsilon^7 + 0.00048069\epsilon^8 + 0.00010791\epsilon^9 + 6.7792 \times 10^{-6}\epsilon^{10} - \\ & 0.000023325\epsilon^{11} - 0.000020161\epsilon^{12} - 3.8825 \times 10^{-6}\epsilon^{13} + 7.1301 \times 10^{-7}\epsilon^{14} + 1.1828 \times 10^{-6}\epsilon^{15} + \\ & 8.9935 \times 10^{-7}\epsilon^{16} + 1.1027 \times 10^{-7}\epsilon^{17} - 9.9766 \times 10^{-8}\epsilon^{18} - 6.0926 \times 10^{-8}\epsilon^{19} - 3.6467 \times 10^{-8}\epsilon^{20} - \\ & 1.5256 \times 10^{-11}\epsilon^{21} + 8.7439 \times 10^{-9}\epsilon^{22} + 2.8529 \times 10^{-9}\epsilon^{23} + 9.8924 \times 10^{-10}\epsilon^{24} - 3.551 \times 10^{-10}\epsilon^{25} - \\ & 6.2361 \times 10^{-10}\epsilon^{26} - 9.9193 \times 10^{-11}\epsilon^{27} + 2.5033 \times 10^{-11}\epsilon^{28} + 3.8338 \times 10^{-11}\epsilon^{29} + 3.6974 \times 10^{-11}\epsilon^{30} \end{aligned}$$

Curves out of $A_0=3/2$:

$$\begin{aligned} \text{Lower } \epsilon A = & \frac{3}{2} - \frac{\epsilon^2}{6} + \frac{109\epsilon^4}{3456} - \frac{3419\epsilon^6}{1990656} - \frac{297305\epsilon^8}{573308928} + \frac{7797193367\epsilon^{10}}{82556485632000} \end{aligned}$$

Lower $\epsilon A =$

$$\begin{aligned}
& 1.5 - 0.16667 \epsilon^2 + 0.031539 \epsilon^4 - 0.0017175 \epsilon^6 - 0.00051858 \epsilon^8 + 0.000094447 \epsilon^{10} + \\
& 0.000013172 \epsilon^{12} - 5.7415 \times 10^{-6} \epsilon^{14} - 1.1848 \times 10^{-7} \epsilon^{16} + 3.354 \times 10^{-7} \epsilon^{18} - 2.8733 \times 10^{-8} \epsilon^{20} - \\
& 1.7574 \times 10^{-8} \epsilon^{22} + 3.7778 \times 10^{-9} \epsilon^{24} + 7.2633 \times 10^{-10} \epsilon^{26} - 3.3523 \times 10^{-10} \epsilon^{28} - 1.1097 \times 10^{-11} \epsilon^{30}
\end{aligned}$$

$$\text{Upper } \epsilon A = \frac{3}{2} + \frac{\epsilon^2}{3} - \frac{53 \epsilon^4}{3456} - \frac{6983 \epsilon^6}{1990656} + \frac{740213 \epsilon^8}{2866544640} + \frac{6745666577 \epsilon^{10}}{82556485632000}$$

Upper ϵA =

$$\begin{aligned}
& 1.5 + 0.33333 \epsilon^2 - 0.015336 \epsilon^4 - 0.0035079 \epsilon^6 + 0.00025822 \epsilon^8 + 0.00008171 \epsilon^{10} - \\
& 0.000015556 \epsilon^{12} - 1.5903 \times 10^{-6} \epsilon^{14} + 1.0185 \times 10^{-6} \epsilon^{16} - 3.4918 \times 10^{-8} \epsilon^{18} - 5.8479 \times 10^{-8} \epsilon^{20} + \\
& 8.9289 \times 10^{-9} \epsilon^{22} + 2.7575 \times 10^{-9} \epsilon^{24} - 9.066 \times 10^{-10} \epsilon^{26} - 8.0056 \times 10^{-11} \epsilon^{28} + 7.1452 \times 10^{-11} \epsilon^{30}
\end{aligned}$$

Curves out of $A_0=4$:

$$\begin{aligned}
\text{Lower } \epsilon A = & 4 - \frac{9 \epsilon^2}{32} - \frac{5 \epsilon^3}{64} + \frac{2877 \epsilon^4}{40960} + \frac{2537 \epsilon^5}{737280} - \frac{54707 \epsilon^6}{15728640} + \frac{11663959 \epsilon^7}{14155776000} - \\
& \frac{17260922723 \epsilon^8}{12683575296000} - \frac{43486217423 \epsilon^9}{1223059046400000} + \frac{2804162996941 \epsilon^{10}}{14611478740992000}
\end{aligned}$$

Lower ϵA =

$$\begin{aligned}
& 4 - 0.28125 \epsilon^2 - 0.078125 \epsilon^3 + 0.070239 \epsilon^4 + 0.003441 \epsilon^5 - 0.0034782 \epsilon^6 + \\
& 0.00082397 \epsilon^7 - 0.0013609 \epsilon^8 - 0.000035555 \epsilon^9 + 0.00019192 \epsilon^{10} - 0.000016118 \epsilon^{11} + \\
& 0.000037433 \epsilon^{12} + 1.4085 \times 10^{-6} \epsilon^{13} - 0.000011912 \epsilon^{14} + 2.053 \times 10^{-7} \epsilon^{15} - 6.2434 \times 10^{-7} \epsilon^{16} - \\
& 6.8113 \times 10^{-8} \epsilon^{17} + 7.0367 \times 10^{-7} \epsilon^{18} + 1.5598 \times 10^{-8} \epsilon^{19} - 4.6186 \times 10^{-8} \epsilon^{20} + 2.0464 \times 10^{-9} \epsilon^{21} - \\
& 3.6947 \times 10^{-8} \epsilon^{22} - 2.1736 \times 10^{-9} \epsilon^{23} + 7.4707 \times 10^{-9} \epsilon^{24} + 9.323 \times 10^{-11} \epsilon^{25} + 1.5107 \times 10^{-9} \epsilon^{26} + \\
& 1.8088 \times 10^{-10} \epsilon^{27} - 6.9398 \times 10^{-10} \epsilon^{28} - 2.4687 \times 10^{-11} \epsilon^{29} - 2.0128 \times 10^{-11} \epsilon^{30}
\end{aligned}$$

$$\begin{aligned}
\text{Upper } \epsilon A = & 4 - \frac{9 \epsilon^2}{32} + \frac{5 \epsilon^3}{64} + \frac{2877 \epsilon^4}{40960} - \frac{2537 \epsilon^5}{737280} - \frac{54707 \epsilon^6}{15728640} - \frac{11663959 \epsilon^7}{14155776000} - \\
& \frac{17260922723 \epsilon^8}{12683575296000} + \frac{43486217423 \epsilon^9}{1223059046400000} + \frac{2804162996941 \epsilon^{10}}{14611478740992000}
\end{aligned}$$

Upper ϵA =

$$\begin{aligned}
& 4 - 0.28125 \epsilon^2 + 0.078125 \epsilon^3 + 0.070239 \epsilon^4 - 0.003441 \epsilon^5 - 0.0034782 \epsilon^6 - \\
& 0.00082397 \epsilon^7 - 0.0013609 \epsilon^8 + 0.000035555 \epsilon^9 + 0.00019192 \epsilon^{10} + 0.000016118 \epsilon^{11} + \\
& 0.000037433 \epsilon^{12} - 1.4085 \times 10^{-6} \epsilon^{13} - 0.000011912 \epsilon^{14} - 2.053 \times 10^{-7} \epsilon^{15} - 6.2434 \times 10^{-7} \epsilon^{16} + \\
& 6.8113 \times 10^{-8} \epsilon^{17} + 7.0367 \times 10^{-7} \epsilon^{18} - 1.5598 \times 10^{-8} \epsilon^{19} - 4.6186 \times 10^{-8} \epsilon^{20} - 2.0464 \times 10^{-9} \epsilon^{21} - \\
& 3.6947 \times 10^{-8} \epsilon^{22} + 2.1736 \times 10^{-9} \epsilon^{23} + 7.4707 \times 10^{-9} \epsilon^{24} - 9.323 \times 10^{-11} \epsilon^{25} + 1.5107 \times 10^{-9} \epsilon^{26} - \\
& 1.8088 \times 10^{-10} \epsilon^{27} - 6.9398 \times 10^{-10} \epsilon^{28} + 2.4687 \times 10^{-11} \epsilon^{29} - 2.0128 \times 10^{-11} \epsilon^{30}
\end{aligned}$$

20 51NFS 1103
In 1/99 22527-157

DUDLEY KNOX LIBRARY



3 2768 00360693 0